# DEVELOPMENT OF UP-CONVERSION NANOPARTICLE-BASED PORTABLE SCREENING TEST FOR DIAGNOSIS OF INFECTIOUS DISEASES

by
Işıl Çakıroğlu

Submitted to Graduate School of Natural and Applied Sciences
in Partial Fulfillment of the Requirements
for the Degree of Master of Science in
Materials and Nanotechnology Engineering

Yeditepe University
2023

DEVELOPMENT OF UP-CONVERSION NANOPARTICLE-BASED PORTABLE SCREENING TEST FOR DIAGNOSIS OF INFECTIOUS DISEASES

APPROVED BY:

Assist. Prof. Dr. Ayşe Dulda …….
(Thesis Supervisor)
(Yeditepe University)

Assist. Prof. Dr. Özgül Gök …….
(Thesis-Co Supervisor)
(Acıbadem Mehmet Ali Aydınlar University)

Assoc. Prof. Dr. Bilge Güvenç Tuna …….
(Yeditepe University)

Prof. Dr. Soner Doğan …….
(Yeditepe University)

Assist. Prof. Dr. Ceyhun Kırımlı …….
(Acıbadem Mehmet Ali Aydınlar University)

DATE OF APPROVAL: …/…/20…

I hereby declare that this thesis is my own work and that all information in this thesis has been obtained and presented in accordance with academic rules and ethical conduct. I have fully cited and referenced all material and results as required by these rules and conduct, and this thesis study does not contain any plagiarism. If any material used in the thesis requires copyright, the necessary permissions have been obtained. No material from this thesis has been used for the award of another degree.

I accept all kinds of legal liability that may arise in case contrary to these situations.

Işıl Çakıroğlu

# ACKNOWLEDGEMENTS

I would like to thank my esteemed advisors who shared their valuable knowledge with me in the realization of my master's thesis, spared their time when I consulted them, and did everything they could to attract my attention with patience. I will always benefit from the valuable information they have given me in my future career. My professors who fulfill their status, Dr. Ayşe Dulda and my co-advisor, I would like to thank Dr. Özgül Gök.

To dear laboratory friend, PhD student Mahla Shahsavar Göçmen who did not spare their support even for a moment during my thesis writing process that we worked together experimentally,

To Yeditepe University Materials and Nanotechnology Engineering and Acıbadem Mehmet Ali Aydınlar University Nanobiotechnology Laboratories, where I spent my experimental processes and whose infrastructure I used, and to TÜBİTAK, which I received support with the project number 20AG011,

And lastly, I would like to thank my family for their financial and moral support throughout my entire life, who have been the biggest support in my every decision and in the whole process of my life.

# ABSTRACT


## DEVELOPMENT OF UP-CONVERSION NANOPARTICLE-BASED PORTABLE SCREENING TEST FOR DIAGNOSIS OF INFECTIOUS DISEASES

This dissertation is concerned with the development and validation of nanotechnological sensor components and platforms for the diagnosis of A-group beta-hemolytic streptococcus using the lateral flow strip (LFA) method. Streptococcus is a common bacterium found in the human flora, especially in the throat and nose, and is prevalent in rural locations where accurate detection may be challenging. LFA is a rapid, simple, and cost-effective biosensor used for the analysis of various samples at the point of care, making it one of the most common biosensors currently available. The main goal of this thesis is to develop an upconversion nanoparticle-based lateral flow assay (UCNP-LFA) for the rapid detection of A-group beta-hemolytic streptococcus. Surface modification of probes with various polymers and conjugating them with disease-specific antibodies (varying concentration), designing the sensor in which disease-specific antibody traps are imprinted onto a membrane are all necessary steps in the development of Lateral Flow Strip units that is performed in this thesis. In addition, optimization of various buffers that allow flow of disease specific antibody-nanoparticle conjugate through the Nitrocellulose Membrane, and optimization of other strip components such as various types of Nitrocellulose Membrane (with varying pore size), conjugation and sample pads, antibodies dispensing speed were investigated. The developed UCNP-LFA samples were characterized by HR-TEM, SEM, XRD, FTIR, DLS, Zeta potential, Uv-Vis spectroscopy, Fluorescent microscope and PL spectroscopy. The UCNP-LFA tests were evaluated for sensitivity, specificity, accuracy, and achieved a value of 73% , 75%, 74% according to the results, respectively.

# ÖZET

## ENFEKSİYON HASTALIKLARININ YERİNDE TANISI İÇİN UP-DÖNÜŞÜMLÜ NANOPARTİKÜL TABANLI TAŞINABİLİR TARAMA TESTİ GELİŞTİRİLMESİ

Bu tez, yanal akış testi (LFA) yöntemi kullanılarak A grubu beta-hemolitik streptokokların teşhisi için nanoteknolojik sensör bileşenlerinin ve platformlarının geliştirilmesi ve doğrulanması ile ilgilidir. Streptococcus, insan florasında, özellikle boğaz ve burunda bulunan yaygın bir bakteridir. Bu bakteri teşhis ve tespitin zor olduğu kırsal bölgelerde yaygındır. LFA, bakım noktasında çeşitli numunelerin analizi için kullanılan hızlı, basit ve uygun maliyetli bir biyosensördür. Sağlık alanındaki gelişmelere bağlı olarak şu anda mevcut olan en yaygın biyosensörlerden biridir. Bu tezin temel amacı, A grubu beta-hemolitik streptokokların hızlı tespiti için up-conversion nanopartikül tabanlı bir yanal akış testi (UCNP-LFA) geliştirmektir. Probların çeşitli polimerlerle yüzey modifikasyonu ve hastalığa özgü antikorlarla (farklı derişimlerdeki konsantrasyonlarda) konjuge edilmesi, hastalığa özgü antikor tuzaklarının bir membran üzerine basıldığı sensörün tasarlanması, bu tezde gerçekleştirilen Yanal Akış Şeridi birimlerinin geliştirilmesinde gerekli adımlardır. Ayrıca, hastalığa özgü antikor-nanopartikül konjugatının Nitroselüloz Membran boyunca akışına izin veren çeşitli tamponların optimizasyonu ve çeşitli Nitroselüloz Membran türleri (değişen gözenek boyutuna sahip), konjugasyon ve numune pedleri, test ve kontrol şeritleri çizmek için tasarlanan cihazda antikor dağıtım hızı gibi diğer şerit bileşenlerinin optimizasyonu araştırılmıştır. Geliştirilen UCNP-LFA örnekleri HR-TEM, SEM, XRD, FTIR, DLS, Zeta potansiyeli, Uv-Vis spektroskopisi, Floresan mikroskop ve PL spektroskopisi ile karakterize edilmiştir. UCNP-LFA testleri duyarlılık, özgüllük ve doğruluk açısından değerlendirilmiş ve sonuçlara göre sırasıyla %73, %75, %74 değerlerine ulaşılmıştır.

# TABLE OF CONTENTS

ACKNOWLEDGEMENTS ..... iv

ABSTRACT ..... v

ÖZET ..... vi

LIST OF FIGURES ..... ix

LIST OF TABLES ..... xii

LIST OF SYMBOLS/ABBREVIATIONS ..... xiv

1. INTRODUCTION ..... 1

2. BACKGROUND ..... 4

2.1. Biosensor Systems ..... 4

2.2. Types of Biosensors ..... 5

2.3. Point of Care Testing ..... 6

2.3.1 Lateral Flow Biosensors ..... 7

2.3.1.1. Sandwich Assay ..... 9

2.3.1.2. Competitive Assay ..... 10

2.4. Uses of Biosensors ..... 11

2.5. Polymeric Nanostructure Materials ..... 13

2.5.1. Nanoparticles ..... 14

2.5.1.1. Up-Conversion Nanoparticles ..... 15

2.6. Surface Functionalization of Materials ..... 16

2.6.1. Polyacrylic Acid (PAA) ..... 16

2.6.2. Dopamin ..... 18

2.7. Antibodies ..... 19

2.7.1. Advantages and Disadvantages of Antibodies ..... 20

2.8. Streptococcus ..... 21

3. MATERIALS AND METHODS ..... 25

3.1. Materials ..... 25

3.2. Synthesis and characterization of UCNP nanoparticles ..... 25

3.3. Synthesis and Characterization of Dopamine-Coated UCNP ..... 26

3.4. Synthesis and Characterization PAA-Coated UCNP ..... 27
3.5. Synthesis and Characterization of Antibody-Conjugated DOPAMIN COATED UCNP ..... 28
3.6. Synthesis and Characterization of Antibody-Conjugated PAA-Coated UCNP ..... 29
3.7. Bacterial Growth ..... 30
3.8. Strip Design Using the Lateral Flow Method ..... 31
3.8.1. Sample Pad ..... 33
3.8.2. Conjugation Pad ..... 34
3.8.3. Membrane ..... 35
3.8.4. Drawing of Antibodies with the Device on the Membrane ..... 38
3.8.5. Absorbent Pad ..... 40
4. RESULTS AND DISCUSSION ..... 41
4.1. Morphological and Structural Characterizations ..... 41
4.1.1. SEM & TEM ..... 41
4.2. Spectroscopic Characterizations ..... 45
4.2.1. DLS & Zeta Potential ..... 45
4.2.2. UV-VIS ..... 50
4.2.4. Photoluminescence Analysis (PL) ..... 55
4.3. Strip Characterization ..... 56
4.3.1. Fluorescent Microscope ..... 56
4.4. Statistical Analysis ..... 62
4.4.1. Sensitivity and Specificity ..... 62
5. CONCLUSION ..... 70
REFERENCES ..... 71

# LIST OF FIGURES

Figure 1. Strip Design Scetch with Autocad Fusion 360 Program ..... 1

Figure 2.1. Components of the biosensor [12] ..... 5

Figure 2.3.1.1 Schematic of the main components and operation of a typical LFA [6]. ..... 8

Figure 2.3.1.2 Advantages and disadvantages of the lateral flow assay [5] ..... 9

Figure 2.3.1.3. (a) Sandwich format lateral flow assay, (b) Competitive format lateral flow assay [18]. ..... 11

Figure 2.5. Polymeric nanostructure materials [27] ..... 13

Figure 2.5.1. Examples of optical readouts of LFAs using different types of nanoparticles [6]. ..... 15

Figure 2.5.1.1 Schematic illustration for various ultrasensitive LFA detection from qualitative to quantitative [29]. ..... 16

Figure 2.6.1.1. Examples of polymers ..... 17

Figure 2.6.1.2. The structure of poly(acrylic acid) (PAA) [41]. ..... 18

Figure 2.6.2.1. Chemical structure of dopamine [44]. ..... 19

Figure 2.8.1. SEM images of group a streptococcus pyogenes interacted with magnetic AuNPs in 40 k magnification [51]. ..... 22

Figure 2.8.3. Estimated global mortality from individual pathogens in 2002 [53]. ..... 24

Figure 3.6.1 Conjugation of the surface of PAA-coated UCNP nanoparticles with biomolecules. ..... 29

Figure 3.7.1. Measurement of Streptococcus samples by Densimeter ..... 31

Figure 3.8.1. An example of a strip design placed in a cabinet ..... 32

Figure 3.8.2. Examples of replicated strip designs ..... 32

Figure 3.8.3 Examples of positive and negative strip designs ..... 33

Figure 3.8.1.1. Sample pads prepared in different parameters. ..... 34

Figure 3.8.2.1. Conjugation pads prepared in different parameters. ..... 35

Figure 3.8.2.2. Incubation of conjugation pads prepared in different parameters. ..... 35

Figure 3.8.3.1 Nitrocellulose membranes with different pore sizes ..... 36

Figure 3.8.3.2 Membranes Product Information ..... 37

Figure 3.8.3.4. Membrane obtained with trehalose solution. ..... 38

Figure 3.8.4.1. (a) Backing card and nitrocellulose membran, (b) Test and control line drawing on the device, (c) Incubation of membranes at 37°C after antibody drawing, (d) nitrosellulose membran after incubation, (e) Membranes that are ready for testing with manual cutting after incubation. ..... 39

Figure 3.8.4.6. Antibody materials used in conjugate pad, test, and control lines [6,55] .... 39

Figure 4.1.1.1. SEM image of NaYF4:Yb, Er nanoparticles ..... 41

Figure 4.1.1.2. (a) TEM image of NaYF4 nanoparticles, (b) histograms of particle size distribution ..... 42

Figure 4.1.1.3. HRTEM image of NaYF4: Yb, Er nanoparticles ..... 42

Figure 4.1.1.4. TEM images of NaYF4:Yb, Er nanoparticles coated with dopamine ..... 43

Figure 4.1.1.5. TEM images of $NaYF_4$:Yb, Er nanoparticles coated with PAA ..... 44

Figure 4.1.2.1. XRD Pattern of NaYF4:Yb, Er ..... 44

Figure 4.2.1.1. (a) Particle size distribution by intensity UCNP-dopamin. (b) Particle size distribution by intensity UCNP-dopamin-antibody conjugation. ..... 45

Figure 4.2.1.2. Particle size distribution by intensity UCNP-PAA-AB. ..... 46

Figure 4.2.1.4. Zeta potential distribution of the; (a) Pure UCNP, (b) Surface modified UCNP with PAA (c) Antibody conjugated UCNP. ..... 49

Figure 4.2.2.1. Uv-vis spectroscopy analysis standart curve with PBS ..... 50

Figure 4.2.3.3. C=O stress region; 1800-1650 cm-1 ..... 54

Figure 4.2.3.4. FT-IR analysis of bare UCNP, PAA and UCNP-PAA-AB ..... 54

Figure 4.2.4.1. PL spectra of the NaYF4 :Yb, Er nanoparticles. There are three emission peaks which are around 521 nm, 545 nm and 660 nm wavelengths. ..... 55

Figure 4.2.4.2. (a) Camera image taken on strip under white light, (b) Camera image under near infrared light, (c) Signals received in spectrophotometer over Test and Control lines. ..... 56

Figure 4.3.1.1. (a) Visualization of the prepared tests under a fluorescent microscope (b) Dyes selected according to the emissions in the microscope used. ..... 57

Figure 4.3.1.2. Visualization of the conjugation pad of the prepared negative tests under a fluorescent microscope. ..... 57

Figure 4.4.1.1. Sensitivity, specificity values formulas [61]. ..... 62

Figure 4.4.1.2. Diagram demonstrating the basis for deriving sensitivity, specificity, and positive and negative predictive values. [61] ..... 63

# LIST OF TABLES

Table 2.3.1. Diagnostics for group a streptococcus [3] ..... 7

Table 2.5. Uses of nanoparticle [30,31] ..... 14

Table 2.7.1. Advantages and disadvantages of antibodies ..... 20

Table 2.8.1 The spectrum of clinical disease caused by the group a streptococcus in children [7]. ..... 22

Table 3.3.1. Calculations of materials used in dopamin coating ..... 27

Table 3.4.1. Calculations of materials used in PAA coating ..... 28

Table 3.5.1. Calculations of materials used in conjugation 1 ..... 29

Table 3.6.1. Calculations of materials used in conjugation 2 ..... 30

Table 3.8.3.1. Membrane models ..... 37

Table 3.8.4.1. Concentrations of antibodies ..... 38

Table 4.2.2.1. Uv-vis spectroscopy analysis results ..... 50

Table 4.3.1.1. (a) Demonstration of test line of prepared positive tests under fluorescence microscope (b) Demonstration of test line of prepared positive tests under fluorescence microscope. ..... 58

Table 4.3.1.2. (a) Demonstration of a negative test prepared under a fluorescent microscope test line. (b1) Demonstration of a negative test prepared under a fluorescent microscope due to the use of high concentration antibodies in the control line. (b2-b3) Demonstration of a negative test prepared under a fluorescent microscope due to the use of low concentration (1:2 ratio) UCNP in the control line at the 30th minute. ..... 60

Table 4.4.1.1. Pathogen Existence ..... 63

Table 4.4.1.2. Results for sensitivity and specificity [56,57]. ..... 64

Table 4.4.1.3. Parameters for LFA strip ..... 64

Table 4.4.1.4. Depending on antibody concentrations ..... 65

Table 4.4.1.5. Depend on membrane pore size..... 66

Table 4.4.1.6. Depending on sample pad thickness..... 66

Table 4.4.1.7. Depending on conjugation pad models..... 68

Table 4.4.1.8. Optimized tests ..... 68

# LIST OF SYMBOLS/ABBREVIATIONS

| | |
|---|---|
| APSGN | Acute post-streptococcal glomerulonephritis |
| ARF | Acute rheumatic fever |
| BSA | Bovine serum albumin |
| DLS | Dynamic light scattering |
| DNA | Deoxyribonucleic acid |
| EDC | 1-ethyl-3-(3-dimethylaminopropyl) carbodiimide |
| $ErCl_3$ | Erbium (III) chloride |
| GAS | Group a streptococcus |
| HCL | Hydrochloric acid |
| LFA | Lateral flow assay |
| NAATS | Nucleic acid amplification tests |
| NaCl | Sodium chloride |
| NaOH | Sodium hydroxide |
| $NH_4F$ | Ammonium fluoride |
| NHS | N-Hydroxysuccinimide |
| PAA | Poly acrylic acid |
| PBS | Phosphate buffer saline |
| PCR | Polymerase chain reaction |
| PD | Polydopamine |
| PDI | Polydispersity |
| POCT | Point of care tests |
| RADTS | Rapid antigen detection tests |
| SEM | Scanning electron microscopes |
| TEM | Transmission electron microscopes |
| THF | Tetrahydrofuran |
| UCNP | Up conversion nanoparticles |
| XRD | X-Ray diffractometer |
| $YbCl_3$ | Ytterbium (III) chloride |
| $YCl_3$ | Yttrium (III) chloride |

# 1. INTRODUCTION

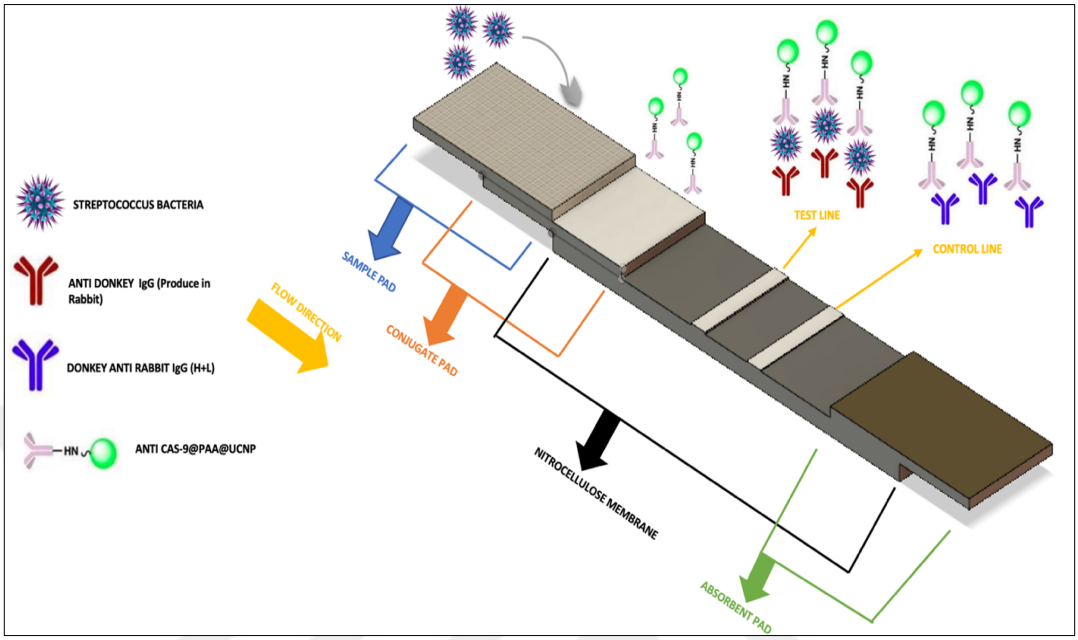


Figure 1. Strip Design Scetch with Autocad Fusion 360 Program

In today's technology, the rapid, cost effective, and efficient identification of disease that affects humans, especially the prompt detection of viruses, bacteria, and parasites within the body, is very crucial. Infectious diseases caused by pathogenic microorganisms pose a significant risk and are highly contagious, which makes them a critical concern for public health and economy [1].

Blood culture, immunoassays, polymerase chain reaction (PCR), mass spectrometry (MS), and genetic sequencing have been used conventionally for diagnosis of viruses, bacteria, and parasites. However, these tests are performed in central clinical laboratories with sophisticated equipment that are costly and require well-trained operators and labor intensive. Therefore, point-of-care testing (POCT) plays an important role in providing timely and accurate results to patients in urban areas where central laboratories are not accessible, and to those who receive home care, enabling quickly delivering results and supporting appropriate treatment [2].

Most studies have reported culture sensitivity of up to 95%, however such tests are performed in clinical reference laboratories with highly standardized processes. These tests

require clinical labs and take a long time to detect bacteria. The need for rapid diagnosis and quick antigen detection, has led to the RADTS development, enabling administration of antibiotics without delaying the treatment. In general, these tests are time-consuming and required to be performed in central clinical laboratories. Apart from that, the laboratories should be well-equipped due to requiring specific devices which are cost effective. Alongside these labor-intensive tests, point-of-care tests (POCT) allow clinical testing to be brought closer to the field of patient care, thanks to recent advances in the biomarker field [3]. By bringing clinical testing closer to the field of patient care, POCTs can provide diagnostic results more quickly, improving the quality of care for both individual patients and the population at large. With these methods, early diagnosis of infectious diseases that threaten the world population will prevent their spread, apart from directing an effective treatment with sensitive and specific diagnostic tests.

Lateral flow assays (LFAs) are a type of Lateral flow systems POCTs that are simple, economic, and user friendly [4]. In LFA systems, analytes such as antibodies are used to detect the bioreceptor in the test line and the control line, and to capture the target molecules between the capture bioreceptor and generate signals. Designing lateral flow tests require different bioreceptors since binding of the target to different epitopes increases the sensitivity of the test. Therefore, two different bioreceptors are needed that bind to different parts of the target molecule. To increase the binding capability of antibodies, polymers are used and covalently linked to the bioreceptors. The purpose of this study is to develop diagnostic tools for detection of a-group beta-hemolytic streptococci using the Lateral Flow Strip (LFA) method [5,6]. Group A beta-hemolytic streptococci (GAS), known as Streptococcus pyogenes, are a type of infectious agent commonly found in children and cause the broadest spectrum of clinical bacterial diseases in children. The most common infections caused by GAS are pharyngitis and pyoderma, which occur in their later stages. However, it also causes skin infections. This disease, which is mostly seen in children aged 5-8 years, triggers many diseases such as acute rheumatic fever, rheumatic heart disease, and invasive infections when its severity increases [7,8].

In this study, dopamine and polyacrylic acid polymer coated up-conversion nanoparticles were produced and conjugated with antibodies in the lateral flow system, comparatively. Dopamine and PAA-coated UCNP nanoparticles are fixed to the conjugate pad after antibody conjugation to design a specific biosensor with high sensitivity to the detection of

streptococcal bacteria. The findings were characterized by various characterization techniques including TEM ,DLS, Zeta potential, FTIR, PL, and Fluorescence microscopy, etc.

# 2. BACKGROUND

In this section, the background of the key concepts of this study such as biosensor systems and the types of it are mentioned.

## 2.1. BIOSENSOR SYSTEMS

A biosensor is a device that detects the presence and activity of biological materials (e.g. proteins, enzymes, DNA and cells) or biological processes such as cell metabolism, enzyme reactions, antigen-antibody interactions, DNA hybridization, and other biological interactions. Biosensors are utilized in various fields due to their advantages such as sensitivity, selectivity, fast response time and portability such as the environment, medicine, food industry, food quality control, and defense. [9,10].

Biosensors commonly include three fundamental components:

1. Bioreceptor,
2. Transducer,
3. Signal Processing.

The bioreceptor element interacts with the biological target analyte and generates a signal as a result of this interaction. This element can usually be an antibody, an enzyme, a DNA probe or a cell surface receptor. The transforming element converts the signal from the biological recognition element into a measurable signal. This element can be an electrochemical, optical, fluid or thermal converter. According to components of biosensors, the label can indeed be considered an example of a transducer. A label is a molecule or entity that is attached to the biological recognition element and is responsible for generating a measurable signal in response to the presence of the target analyte. The label acts as a transducer by converting the biochemical or biophysical interaction between the recognition element and the analyte into a detectable signal, such as an electrical, optical, or thermal signal. Common examples of labels used in biosensors include enzymes, fluorophores, and nanoparticles. The label's signal is then detected and quantified by the transducer of the biosensor to provide information about the presence and concentration of the target analyte. The reading part signal is where the response can be visually observed [9,11,12,13].

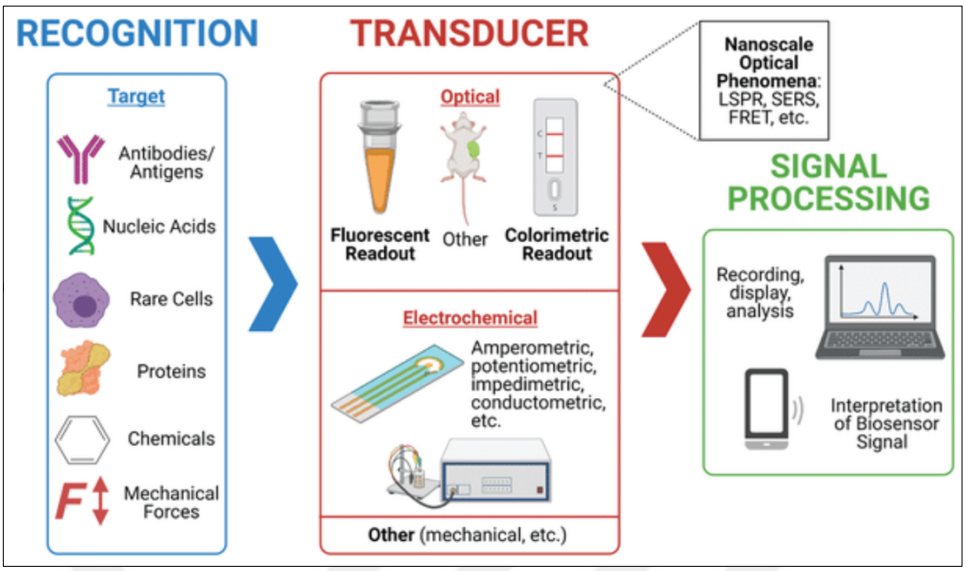


Figure 2.1. Components of the biosensor [12]

## 2.2. TYPES OF BIOSENSORS

Biosensors classifies based on the type of biological recognition element [11]:

**a. Enzyme-based biosensors:** These biosensors use enzymes as their biological recognition element, which catalyze the reaction of the analyte and produce a detectable signal.

**b. Antibody-based biosensors:** These biosensors use antibodies as their recognition element, which specifically bind to the analyte of interest.

**c. Nucleic acid-based biosensors:** These biosensors use nucleic acids such as DNA or RNA as their recognition element, which bind to complementary sequences of the analyte.

Biosensors based on the type of transducer:

**a. Electrochemical biosensors:** These biosensors use electrical signals to measure the analyte.

**b. Optical biosensors:** These biosensors use light to measure the analyte.

**c. Piezoelectric biosensors:** These biosensors use mechanical signals to measure the analyte.

Biosensors based on the location of the biosensor [14,15]:

**a. Implantable biosensors:** These biosensors are implanted in the body and monitor physiological parameters in real-time.

**b. Wearable biosensors:** These biosensors can be worn on the body and monitor physiological parameters in real-time.
**c. Point-of-care biosensors:** These biosensors are designed for use at the point-of-care, such as in a doctor's office or a home.

There are also other ways to classify biosensors, such as based on the type of sample, the specificity of the recognition element, and the range of detection among others.

## 2.3. POINT OF CARE TESTING

POCT refers to medical diagnostic testing that is performed at or near the patient's location, as opposed to the traditional laboratory testing that requires samples to be sent to a central laboratory for analysis. POCT devices and test kits are designed to be portable, easy-to-use, and provide rapid diagnostic results that can be used to guide medical decision-making and treatment. POCT can be used for a wide variety of medical tests, including blood glucose monitoring, cholesterol testing, pregnancy testing, rapid strep tests, and many others [2].
Point of care tests are commonly available in hospital emergency rooms, clinics, doctor's offices, and even in patients' homes. The advantages of POCTs include faster turnaround times for results, POCT can provide results within minutes, whereas traditional laboratory testing can take several hours or even days. More efficient use of resources: POCT eliminates the need for samples to be sent to a central laboratory for analysis, which can save time and money. Improved patient outcomes: Rapid diagnostic results from POCT can help healthcare providers make more timely and accurate diagnoses and treatment decisions, which can improve patient outcomes [16].

Bacteria detecting with different methods such as culture, RADTs and 3- Molecular POCTs. Culture testing is a bacterial culture that is considered the gold standard in the diagnosis of GAS due to its high sensitivity and specificity. Positive cultures take 18 to 24 hours , while negative cultures take 24 to 48 hours. Culture sensitivity has been reported in a high value of 95%, however most of these studies were performed in clinical reference laboratories with highly standardized processes. The disadvantages of these tests are that they need to be performed in clinical laboratories and bacteria detection time is too long. Second is RADTs, the evolving clinical need for rapid diagnosis and rapid antigen detection has led to the

development of tests. Thus, it is ensured that antibiotics can be administered without delay. Finally molecular POCTs are due to the lower sensitivities of RADTs and the need to treat patients based on diagnostic results, nucleic acid amplification tests (NAATs) have been developed for the detection of GAS. However, it needs to be a clinical environment [3].

Table 2.3.1. Diagnostics for group a streptococcus [3]

| 1- Culture | 2- RADTs | 3- Molecular POCTs |
|---|---|---|
| | a) Latex agglutination assays<br>b) LFIAs<br>c) OIAs | a) Roche cobas strep A assay.<br>b) Abbott strep A and strep A2 assays.<br>c) Xpert Xpress strep A assay. |

### 2.3.1 Lateral Flow Biosensors

Lateral Flow Assay (LFA) is a simple and rapid diagnostic test that is used to detect the presence or absence of a target analyte in a sample that is known as a lateral flow immunoassay or a strip test. LFAs are often used for point-of-care testing, where detections are quick and without requiring specialized equipment or technical expertise [5,17].

The LFA consists of a small plastic strip or card that includes a sample pad, a conjugate pad, a test line, and a control line. The sample pad is where the specimen, such as blood or urine, is added to the test. The conjugate pad contains a labeled reagent, such as a gold nanoparticle or an enzyme, that is specific to the target analyte. The test line contains an immobilized capture reagent, such as an antibody or aptamer, that is specific to the target analyte. On the

other hand, the control line contains a similar immobilized capture reagent, similar to the test line, but it is not bound to the target analyte [5,18].

As the specimen is added to the sample pad, it flows through the conjugate pad and interact with the labeled reagent. If the target analyte is present in the sample, it binds to the labeled reagent, forming a complex. The complex then flows along the test and is captured by the immobilized capture reagent at the test line, causing a visible line to appear. The control line serves as a positive control, indicating that the assay has worked correctly. LFAs are easy to use, do not require specialized equipment, and can provide results in a matter of minutes. They are widely used in clinical settings, as well as in environmental testing, food safety, and other applications where rapid and reliable testing is needed [5].

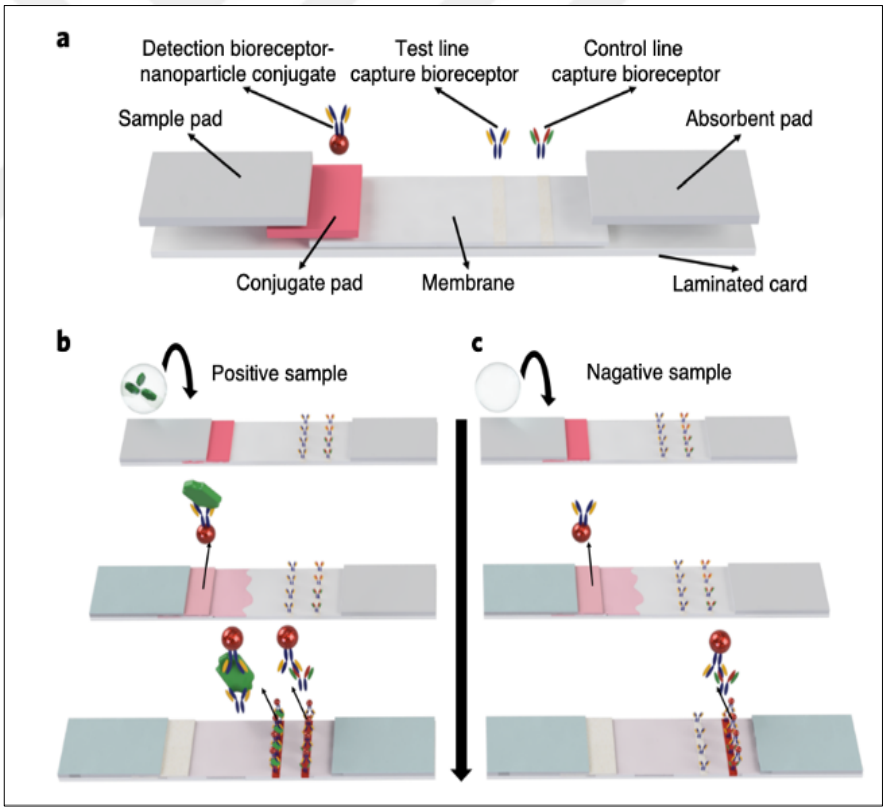


Figure 2.3.1.1 Schematic of the main components and operation of a typical LFA [6].


Figure 2.3.1.2 Advantages and disadvantages of the lateral flow assay [5]

### *2.3.1.1. Sandwich Assay*

A sandwich assay is a type of immunoassay used to detect and quantify the amount of a specific antigen or protein in a sample. This assay relies on the use of two different antibodies, which sandwich the target antigen or protein between them, hence the name.In this detection method. The first antibody, called the capture antibody, is immobilized onto a solid surface, such as the surface of a microplate well. The sample containing the target

antigen or protein is then added to the well, allowing the antigen or protein to bind to the capture antibody [18]. After washing away any unbound sample components, a second antibody, called the detection antibody, is added to the well. This detection antibody is labeled with a detectable marker, such as an enzyme or a fluorescent molecule. The detection antibody binds to a different part of the target antigen or protein than the capture antibody, effectively sandwiching the target molecule between the two antibodies. Any unbound detection antibody is then removed by washing, and a substrate for the detectable marker is added. The enzyme converts the substrate into a detectable signal, or the fluorescent molecule is excited with a specific wavelength of light to emit fluorescence. The degree of sign or fluorescence is proportional to the quantity of goal antigen or protein gift withinside the sample. Sandwich assays are highly sensitive and specific and can detect very low levels of antigen or protein in a sample. They are commonly used in research and diagnostic settings to detect biomarkers of disease, monitor therapeutic treatments, and assess the efficacy of vaccines [19].

#### *2.3.1.2. Competitive Assay*

A competitive assay is a type of immunoassay used to measure the amount of a specific antigen or analyte in a sample. In this type of assay, a labeled version of the analyte is added to the sample along with an unlabeled version of the analyte, which competes with the labeled analyte for binding to a specific antibody. The sample is incubated with a known amount of the labeled analyte and a limited amount of the antibody that specifically binds to the analyte. The unlabeled analyte withinside the pattern then competes with the categorized analyte for binding to the antibody. The amount of labeled analyte bound to the antibody is inversely proportional to the concentration of the unlabeled analyte in the sample. After incubation, the antibody-bound labeled analyte is separated from the unbound analyte, and the amount of labeled analyte is quantified by measuring the label signal [18]. A decrease in signal indicates that more unlabeled analyte was present in the sample, competing with the labeled analyte for binding to the antibody. Competitive assays are often used to detect small molecules, such as drugs or hormones, in biological samples, such as blood or urine. They are highly sensitive and specific and can detect very low levels of analyte in a sample [20].

The main difference between these two assays is the way in which the target antigen or protein is detected. In a sandwich assay, two different antibodies are used to bind to the target

antigen or protein, effectively sandwiching it between the two antibodies. In a competitive assay, a labeled antigen or protein competes with the unlabeled target antigen or protein in the sample for binding to a limited amount of immobilized antibody.

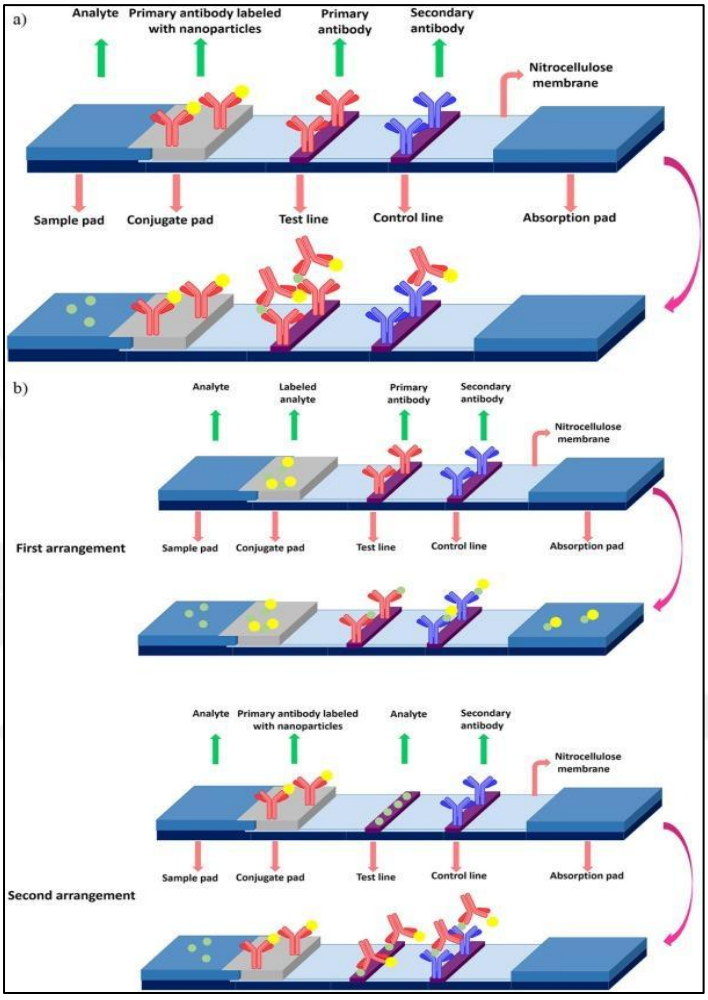


Figure 2.3.1.3. (a) Sandwich format lateral flow assay, (b) Competitive format lateral flow assay [18].

## 2.4. USES OF BIOSENSORS

Biosensors are widely used in various fields due to their ability to detect and analyze biological and biochemical signals. Some of the common uses of biosensors have been listed below.

**Medical diagnostics:** Biosensors play a very important role in medical diagnostics as they detect biomarkers in body fluids or tissues. They can be used to monitor glucose levels in

diabetes, identify infectious pathogens, measure the levels of certain hormones, analyze genetic material, and monitor drug levels in the blood [10,14].

**Environmental Monitoring:** Biosensors can be used to monitor pollutants and contaminants in the environment. They can detect heavy metals, pesticides, toxins and other pollutants in the air, water or soil. This information is used to assess the quality of the environment and ensure public safety [21].

**Food Safety and Quality Control:** Biosensors can be used to detect and quantify food contamination or pathogens. They can detect allergens, bacterial contamination, pesticide residues and decomposition products. Biosensors help prevent foodborne diseases and protect consumer health by ensuring food safety and quality control [10,22].

**Livestock Monitoring:** Biosensors allow farmers and ranchers to monitor crop health, soil conditions, and animal welfare. You can detect nutrient deficiencies, pests and diseases in crops and monitor animal health parameters such as temperature, heart rate and milk composition [23].

**Bioprocess monitoring:** Biosensors are used to monitor and control bioprocesses in the biotech and pharmaceutical industries. Moreover, It is possible to measure parameters such as pH measurement, temperature, dissolved oxygen, metabolite concentrations and biomass density during fermentation processes. This knowledge is used to optimize production and preserve product quality [24].

**Wearables:** Biosensors built into wearables like fitness trackers and smartwatches can monitor vital signs including heart rate, and blood pressure. They provide real-time health information, helping people track fitness goals, manage stress, and track chronic conditions [15].

**Forensic analysis:** Biosensors are used in forensic science to detect and analyze biological evidence such as DNA, blood, saliva or fingerprints. It provides fast and accurate analysis, assists with forensic investigations and obtains evidence in court [25].

**Biosafety and Security:** Biosensors can be used for early detection of biological hazards and bioagents in security environments. They play an important role in biosecurity by monitoring the presence of pathogens, toxins, or biological hazards in different environments. For example, some studies have been done in detecting biological weapons and determining the etiology of infectious diseases [26].

## 2.5. POLYMERIC NANOSTRUCTURE MATERIALS

Polymeric nanostructured materials (PNMs) have been increasingly developed and used in nanosciences, nanotechnology applications, tissue engineering, biomedicine and chemistry, especially in the diagnosis and treatment of diseases. Polymeric nanostructured materials can be designed as nanoparticles, nanogels, nanotubes, nano capsules, nanofibers, micelles and dendrimers. In addition, their stability, quantum size, shape, surface charge, surface chemistry, mechanical strength, porosity and similar properties can be tailored to specific functions. However, once these materials are designed, before using them in applications, it is necessary to perform an effective surface modification to increase their chemical stability, improve their dispersibility in liquid solutions, provide specific surface functionalities with desired biocompatibility and specific affinity, and electronically isolate the nanomaterials from the outside. In order to use these materials for surface modification, first of all, water dispersibility and biocompatibility should be evaluated [27,28].

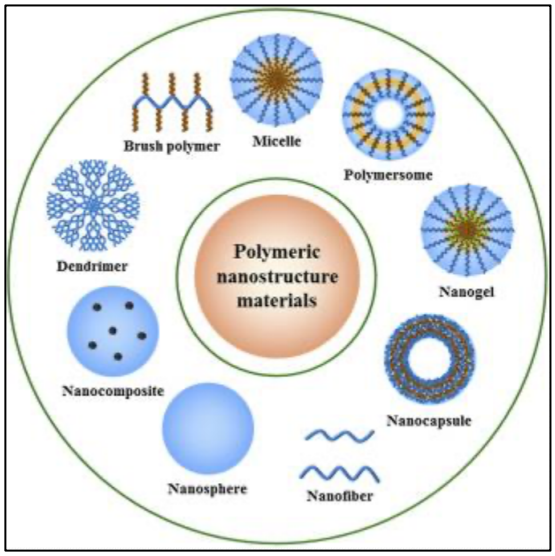


Figure 2.5. Polymeric nanostructure materials [27]

### 2.5.1. Nanoparticles

Nanoparticles are defined as particles with dimensions typically in the range of 1-100 nanometers (nm) that can be obtain from a variety of materials, including metals, semiconductors, polymers, ceramics, and composites. Nanoparticles have unique properties that differ them from their bulk counterparts due to their small size and high surface area-to-volume ratio.

Nanoparticles have a wide range of applications in various fields, including medicine, electronics, energy, and environmental remediation [29,30,31]. Some of the properties of nanoparticles that make them useful in these applications mentioned in the following table.

Table 2.5. Uses of nanoparticle [30,31]

| | |
|---|---|
| **1. Enhanced Surface Area** | Due to their small size and high surface area-to-volume ratio, nanoparticles have a large surface area that can be used for chemical reactions, adsorption, or sensing. |
| **2. Optical and Electronic Properties** | Some nanoparticles exhibit unique optical and electronic properties that can be exploited for sensing, imaging, or electronics applications. For example, gold nanoparticles exhibit strong absorption and scattering of light, making them useful in biosensing and imaging applications. |
| **3. Magnetic Properties** | Some nanoparticles, such as iron oxide nanoparticles, exhibit magnetic properties that can be used for separation, imaging, or drug delivery applications |

| | |
|---|---|
| **4. Controlled Release** | Nanoparticles can be engineered to release their contents in a controlled manner, making them useful for drug delivery and gene therapy applications. |
| **5. Biocompatibility** | Some nanoparticles, such as liposomes or dendrimers, are biocompatible and can be used in biomedical applications. |

However, nanoparticles can also pose some potential risks, particularly if they are not properly characterized, handled, or disposed of. Some nanoparticles may be toxic, reactive, or may have unintended effects on the environment or human health. As a result, it is important to carefully consider the potential risks and benefits of nanoparticles in any application.

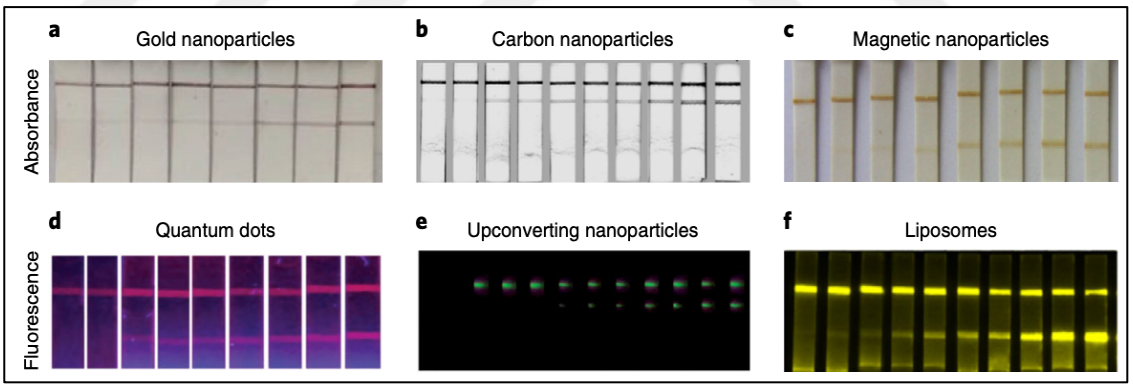


Figure 2.5.1. Examples of optical readouts of LFAs using different types of nanoparticles [6].

### *2.5.1.1. Up-Conversion Nanoparticles*

Up-conversion nanoparticles (UCNPs) are a shape of nanomaterial that could convert low-electricity photons into high-electricity photons through a process called up-conversion. This process involves the absorption of two or more low-energy photons, which are then combined to generate a higher-energy photon with a shorter wavelength [31,32]. UCNPs are typically made up of inorganic materials, such as rare-earth metals, that have unique optical

properties that make them suitable for a variety of applications, including bioimaging, sensing, and drug delivery. One of the key advantages of UCNPs is their ability to emit light in the visible and near-infrared regions of the spectrum, which can penetrate deeper into tissues and provide higher resolution images than traditional fluorescence imaging methods. UCNPs can also be functionalized with a variety of biomolecules, such as antibodies or aptamers, to target specific cells or biomolecules. This makes them useful for targeted imaging and drug delivery applications [33]. In addition, UCNPs have high photostability, low toxicity, and can be synthesized with a range of sizes and shapes, allowing for tailored properties and improved performance. Overall, UCNPs hold great promise for a wide range of biomedical and technological applications, and research in this area is ongoing [34].

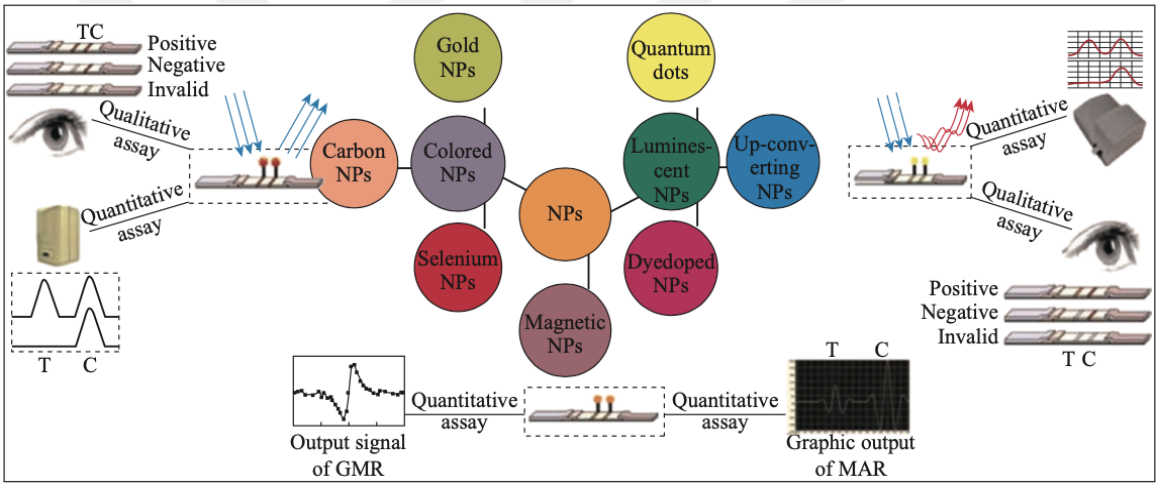


Figure 2.5.1.1 Schematic illustration for various ultrasensitive LFA detection from qualitative to quantitative [29].

## 2.6. SURFACE FUNCTIONALIZATION OF MATERIALS

### 2.6.1. Polyacrylic Acid (PAA)

Polymers are vast molecules consisting, repeated subclasses called monomers. They are formed in a process called polymerization, in which monomers chemically combine into long chains or networks. The word "polymer" comes from the Greek words "poly" meaning many and "meros" meaning parts or units. Polymers are found in a variety of natural and synthetic materials. Natural polymers occur in nature and include substances such as

proteins, DNA and cellulose. On the other hand, synthetic polymers are man-made and have a wide range of uses. Examples of synthetic polymers are plastics, synthetic fibers, adhesives, coatings and many other materials that we encounter in our daily lives. The properties of polymers can vary significantly depending on their chemical structure, the arrangement of the monomers, and the presence of additional components or modifications. This versatility allows polymers to exhibit a wide range of properties such as flexibility, strength, heat resistance, electrical conductivity, and chemical resistance. Polymers can be tailored to specific needs by adjusting their composition and processing techniques. Due to their unique properties, polymers have numerous applications in drug delivery, tissue engineering, tissue adhesive, biosensor and healthcare. The study and development of polymers fall under the field of polymer science or polymer chemistry, which involves understanding their synthesis, structure, properties, and processing methods [35,36,37].

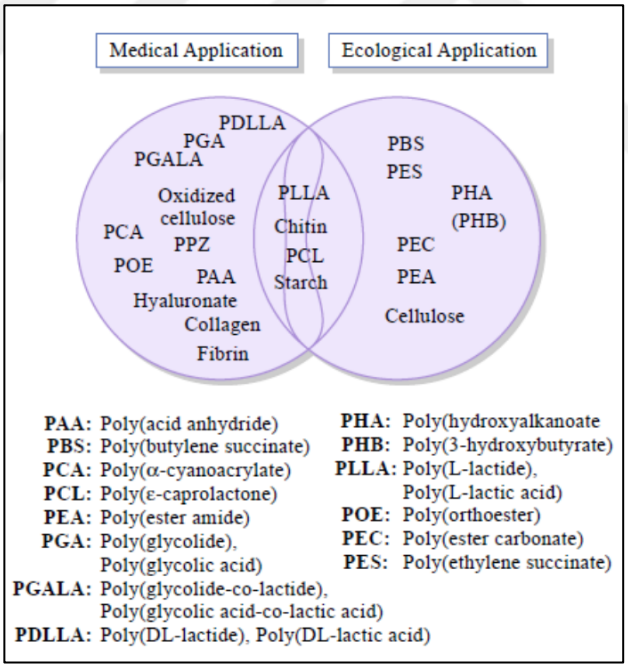


Figure 2.6.1.1. Examples of polymers

Polyacrylic Acid is a synthetic polymer derived from acrylic acid, a monomer with a carboxylic acid function. Polyacrylic acid's ability to absorb water, allowing it to swell and hold large volumes of liquid, makes it ideal for these absorbent applications. In addition, polyacrylic acid has adhesive and thickening properties. The ability to form a strong bond between surfaces makes it useful for different applications [38]. Polyacrylic acid can also be

used as a thickening agent in personal care products such as emulsions, creams and gels. The addition of synthetic polymers can increase the viscosity and stability of products, preventing ingredient separation and providing the desired composition [39]. On the other hand, polyacrylic acid is used as a flotation agent in water treatment processes that collect and precipitate suspended particles in wastewater or industrial water. In general, poly acrylic acid is a versatile polymer with many applications, mainly due to its hydrophilic, adhesion, thickening, and flocculation properties [35,40].

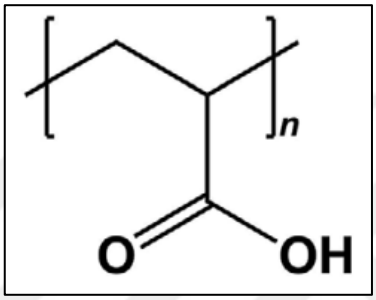


Figure 2.6.1.2. The structure of poly(acrylic acid) (PAA) [41].

**2.6.2. Dopamin**

Dopamine is a biomolecule applied for the surface coatings purposes in various fields of biomaterial. In particular, this coating can increase the adhesion of cells and tissues on the surface, thus promoting cell growth and tissue regeneration in implants and medical devices [42]. The binding of dopamine to the surface depends on the structure of the surface of the coated nanomaterial as well as the structure of the dopamine molecule itself. For example, the hydrophilic or hydrophobic nature of dopamine-coated nanoparticles depends on the method used for coating the nanoparticle with dopamine. Also, the properties of the dopamine coated surface are affected by the choice of solvents and chemicals used in the dopamine coating process, as well as their concentrations. Some studies reported that as dopamine polymerizes it converts to a complex structure poly-dopamine (PD). PD has been found to have a wider range of applications than dopamine. Which is why it is more commonly used for surface coating in research studies. [42,43].

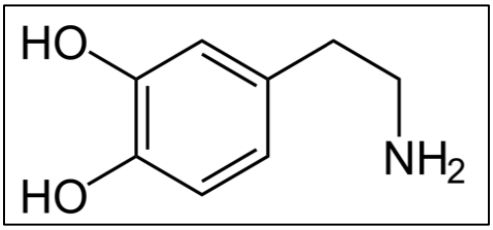


Figure 2.6.2.1. Chemical structure of dopamine [44].

## 2.7. ANTIBODIES

Antibodies are Y-shaped proteins produced by the immune system to recognize, bind, and neutralize foreign substances, such as viruses, bacteria, or toxins. They are also known as immunoglobulins and are produced by specialized white blood cells called B cells. Each antibody is specific to a particular antigen, which is a molecule on the surface of a foreign substance. Antibodies recognize and bind to antigens through their variable regions, which are located at the tips of the Y-shaped structure.

There are five different classes of antibodies: IgM, IgG, IgA, IgE, and IgD. IgM is the first antibody produced in response to an antigen, and it is usually followed by IgG, which Is the maximum ample antibody withinside the blood and may pass the placenta to offer immunity to the growing fetus. IgA is found in secretions such as tears, saliva, and breast milk, and provides protection against pathogens at mucosal surfaces. IgE is involved in allergic reactions, while IgD has a less well-defined function [16,45,46].

Antibodies play a crucial role in the immune response by marking foreign substances for destruction by other immune cells, such as macrophages or natural killer cells. They can also neutralize viruses or toxins by preventing them from binding to host cells.

Antibodies are used extensively in research and medicine, such as in diagnostic tests, therapeutic treatments, and vaccine development. Monoclonal antibodies, which are antibodies produced from a single type of B cell, are widely used in cancer treatments and other diseases [47].

### 2.7.1. Advantages and Disadvantages of Antibodies

Antibodies provide a highly specific and sensitive tool for the detection of target analytes in biosensors, making them a valuable component of many biosensing platforms for clinical, environmental, and industrial applications. While antibodies are a valuable tool in biosensors, their limitations must be carefully considered in the design and development of biosensing assays. Alternative technologies, such as aptamers, peptides, or molecularly imprinted polymers, may be more suitable in some applications.
Antibodies have several advantages in biosensors, including [48]:

Table 2.7.1. Advantages and disadvantages of antibodies

| **Advantages** | **Disadvantages** |
|---|---|
| **1. High specificity:** Antibodies have high specificity for their target antigens, which enables them to distinguish between closely related molecules. This makes them useful in detecting specific proteins, pathogens, and biomolecules in complex biological samples. | **1. Cost:** Antibodies can be expensive to produce and purify, particularly when large quantities are required. This can limit their use in some applications. |
| **2. Sensitivity:** Antibodies can detect very low levels of antigens, making them highly sensitive. This is important in diagnostic applications where the presence of small amounts of an antigen can indicate disease. | **2. Stability:** Although antibodies are generally stable, they can lose activity over time, particularly if not stored properly. This can affect the reliability and accuracy of biosensing assays. |
| **3. Versatility:** Antibodies can be engineered and modified to suit specific biosensing applications, such | **3. Cross-reactivity:** Antibodies can sometimes cross-react with other molecules that are similar in structure to their target |

| | |
|---|---|
| as conjugation with enzymes, fluorescent dyes, or other reporter molecules. This enables the detection of the target analyte in a variety of different formats. | antigen. This can result in false positives or false negatives in biosensing assays. |
| **4. Reproducibility:** Antibodies can be produced in large quantities with high reproducibility, ensuring consistent performance in biosensing applications. | **4. Batch-to-batch variability:** Antibody production can vary from batch to batch, which can affect the performance and consistency of biosensing assays. |
| **5. Stability:** Antibodies are stable under a wide range of conditions, including temperature, pH, and ionic strength. This makes them suitable for use in various biosensing platforms and environments. | **5. Limited shelf life:** Antibodies have a limited shelf life, particularly when used in biosensors. This can limit their use in certain applications where long-term stability is required. |

## 2.8. STREPTOCOCCUS

Group A beta-hemolytic streptococcus (GAS) is a species of bacteria belonging to the genus streptococcus, a group of gram-positive, non-motile, spherical-shaped bacteria. Most require additional media (blood agar). Group A streptococci have a capsule of hyaluronic acid. This is the basic outer cell antigenic structure of group A streptococci. It contains streptococcal superantigen, streptococcal complement inhibitor, cell wall-bound proteins that help bind to human cells, and 2 secreted enzymes with specific effects on IgG [7]. There are many different strains of Streptococcus, some harmless to humans and some that can cause serious infections. Some of these species have common infective agents in children. For this reason, it has the widest range of clinical diseases in children, especially in the 5-14 age range. This disease can be divided into four diseases. These; spectrum is superficial infection, invasive disease, toxin-mediated and post-infectious sequelae diseases (table 2.10.1) [7,49]. For example, the most common diseases seen in children are pharyngitis and pyoderma due to

streptococcal bacteria. Apart from this, invasive diseases are less common than other categories, but this type of disease has a high mortality rate and long-term morbidity. Streptococcal bacteria are commonly found in the human respiratory tract, but they can also be found on the skin, gastrointestinal tract, and other parts of the body. Some types of Streptococci can cause a range of infections, including strep throat, pneumonia, meningitis, sepsis, and skin infections. Streptococcal bacteria are typically spread from person to person through contact with respiratory secretions such as saliva or mucus. Treatment of streptococcal infections may include antibiotics, and severe cases may require hospitalization [50,51].

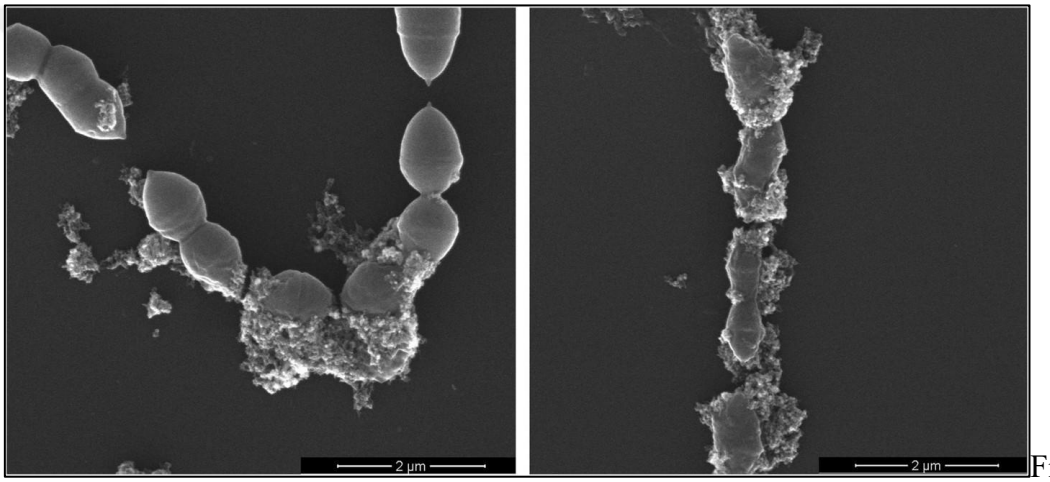


Figure 2.8.1. SEM images of group a streptococcus pyogenes interacted with magnetic AuNPs in 40 k magnification [51].

Table 2.8.1 The spectrum of clinical disease caused by the group a streptococcus in children [7].

| | |
|---|---|
| 1. **Superficial Infection** | a) Pharyngitis and pharyngotonsillitis<br>b) Pyoderma |
| 2. **Invasive Disease** | a) Bacteraemia/septicaemia<br>b) Skin/soft tissue suppurative disease<br>c) Suppurative respiratory disease<br>d) Central nervous system |

| | |
|---|---|
| 3. **Toxin Mediated Disease** | a) Scarlet fever<br>b) Streptococcal toxic shock syndrome |
| 4. **Post-Infectious Sequelae** | a) Rheumatic fever<br>b) Acute post-streptococcal glomerulonephritis<br>c) Reactive arthritis<br>d) Erythema nodusum |

There is a need for fast, inexpensive and effective screening kits that can be used without specializing in rural areas and home care services where access to central laboratories is limited. There is a growing need to prevent the rapid spread of such bacteria worldwide. The reason why GAS infection is a global cause is that it is associated with post-infection autoimmune sequelae, acute rheumatic fever (ARF) and acute post-streptococcal glomerulonephritis (APSGN)-related morbidity and mortality [52]. An estimated 18 million people worldwide currently have a serious case of GAS, with more than 1.7 million new patients. It estimates that at least 517,000 deaths are due to serious GAS diseases (eg, rheumatic fever, rheumatic heart disease, poststreptococcal glomerulonephritis, and invasive infections) each year. The biggest burden is rheumatic heart disease, with a prevalence of at least 15.6 million cases with 282,000 new cases and 233,000 deaths per year. More than 600 million new cases of pyoderma and GAS pharyngitis per year. 3rd ARF outbreaks and increased incidence reports. The prevalence of invasive disease in industrialized countries since the 1980s has highlighted that GAS is a cause of disease in children in these regions. However, the burden of severe GAS disease is predominantly in poor populations living in developing countries and rich countries. Additionally, the minimum estimate of more than 500,000 deaths per year places GAS among the major human pathogens, surpassed only by HIV, Mycobacterium tuberculosis, Plasmodium falciparum and Streptococcus, and is comparable to rotavirus, measles, Haemophilus influenzae type b and possibly (figure 2.10.3) [52,53].

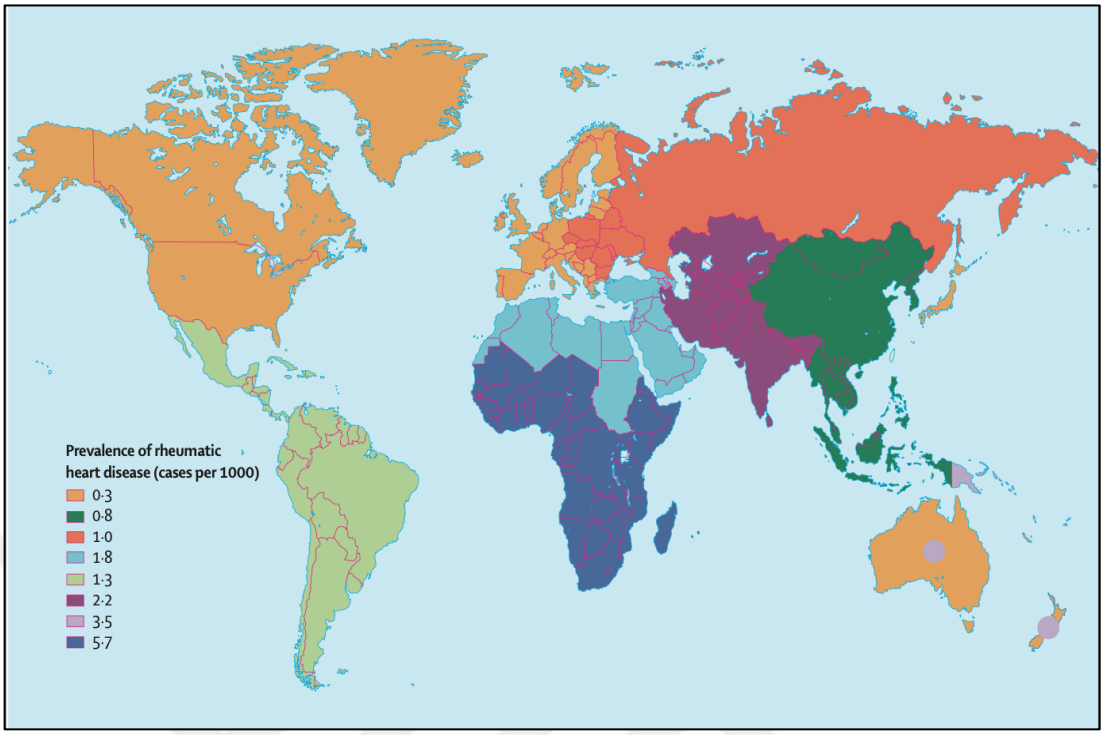


Figure 2.8.2. Prevalence of rheumatic heart disease in children aged 5–14 years [53].

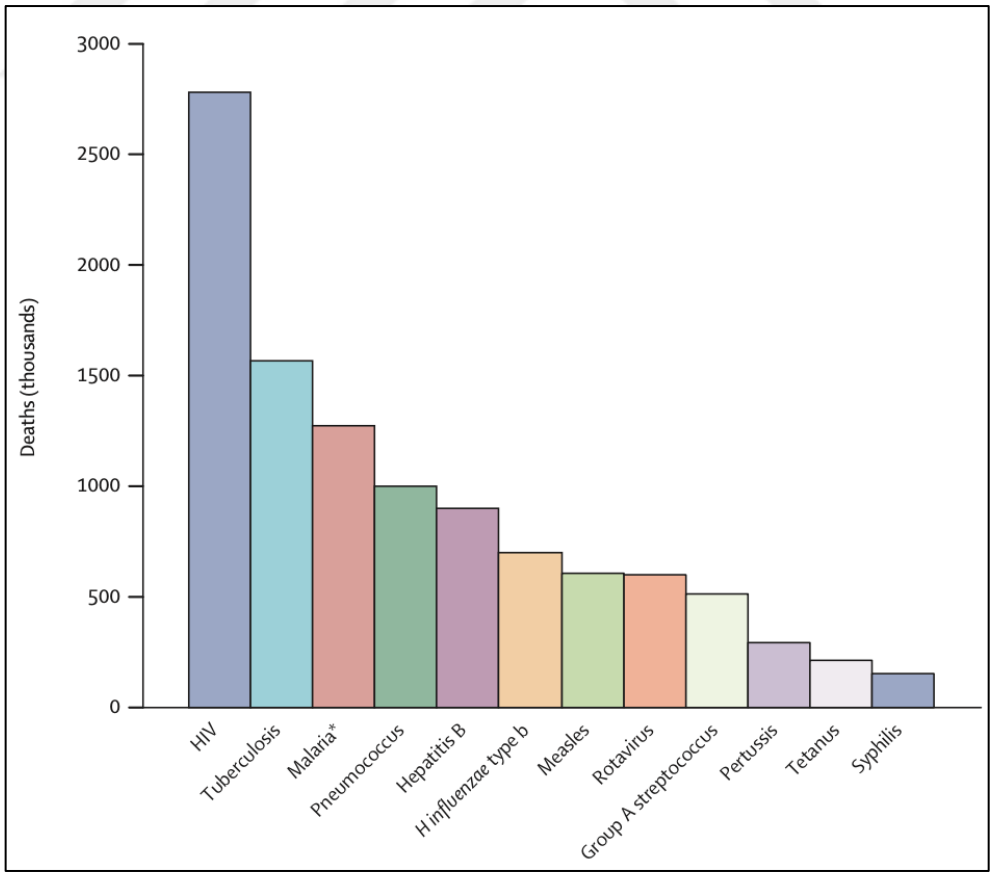


Figure 2.8.3. Estimated global mortality from individual pathogens in 2002 [53].

# 3. MATERIALS AND METHODS

In this section, the materials used in the study and the methodology will be described.

## 3.1. MATERIALS

All chemicals used in the study were obtained from Sigma-Aldrich. The Up-Conversion nanoparticles were synthesized by PhD student Mahla Shahsavar Göçmen in Yeditepe University (Istanbul, Turkey). The antibody used in the biosensor was determined by selecting Anti-Cas 9, the primary antibody that specifically binds to the streptococcus bacteria and whose biological source is rabbit. Streptococcus pyogenes was used as reference bacteria in the study.

## 3.2. SYNTHESIS AND CHARACTERIZATION OF UCNP NANOPARTICLES

As prepared upconversion nanoparticles (NaYF 4 :Yb 3+ , Er 3+) were synthesized by the thermal decomposition technique. The NaYF: Yb Er nanoparticles were prepared by aqueous lanthanide chloride (Ln = 78% Y 3+ , 20% Yb 3+ , 2% Er 3+) adding to the mixture of (6ml) oleic acid and (15ml) octadecene. The mixture was heated to 150ºC for 30 mins and cooled to room temperature. Next step, 10 ml methanol solution of (2.5mmol) NaOH and (4 mmol) NH4F put into the solution while stirring. In the following, the mixture was kept at 60ºC for 30 mins and the reaction was heated to 110ºC and kept for 20 mins under a vacuum to evaporate methanol. Afterward, the temperature set to 300ºC under an argon flow and kept for 1.5h. The resulting nanoparticles were precipitated and washed several times adding ethanol and then collected using centrifugation. Finally, the obtained nanoparticles were dispersed in cyclohexane.

In the next step, structural, particle size, morphology, and optical characterization of the prepared nanoparticles is performed by XRD,DLS,TEM, and PL Spectroscopy.

### 3.3. SYNTHESIS AND CHARACTERIZATION OF DOPAMINE-COATED UCNP

Figure 3.3.1. Dopamine-coated UCNP reaction

Dopamine was dissolved in 50 mg and 300 µl of distilled water. 4.7 ml of tetrahydrofuran (THF) was added to the flask and this mixture was stirred at 50°C under nitrogen gas. UCNPs (15 mg) dissolved in THF (2 ml) were added to this mixture and incubated at 50°C for 5 hours. After 5 hours, UCNP and dopamine were dissolved by adding 100 µl of HCL. Dialysis was applied to the coated UCNPs 3 times with a 1 Kd membrane for 5 hours at room temperature, but it was not successful due to the size of the nanoparticles. For this reason, the nanoparticles that were not subjected to the dialysis process were washed 3 times at 20,000 rpm and precipitated by centrifugation.

In the coating process, 15 mg UCNP + 50 mg Dopamine was used. When UCNPs are used in solvent, the concentration is 7.79 mg per 1 ml. For the experiment a volume of 1.92 ml was used to achieve 15 mg.

Dimensional analysis of the pavement was done with DLS. Since the particle size was high, sonication was performed for 10 minutes. Analysis of surface charges was determined by

Zeta. This process was performed three times. The characterization of dopamine bound to the surface of the particles was determined by FT-IR. Purely synthesized UCNPs and dopamine-coated UCNPs were characterized and analyzed. The morphology of UCNPs and dopamine coated UCNPs was determined by TEM. Finally, dopamine binding to the surface of UCNP nanoparticles was determined by UV-ViS absorption spectrometry. Later, 3 mg of the mixture was dissolved in 300 µl of PBS.

PBS measurement was taken. Samples were prepared by diluting 10 standard curves with 8 mg and 8 ml PBS.) Then the coated solution was measured.

Table 3.3.1. Calculations of materials used in dopamin coating

| **Chemicals** | **eq** | **Mwt (g/mol)** | **n(mmol)** | **Amount(mg)** | **Volume/ ml** |
|---|---|---|---|---|---|
| Dopamin | 1 | 153.18 | 3.06 | 50 | |
| UCNP | 0.3 | | | 15 | |
| THF | | | | | 4.7 |
| HCL | | | | | 100 µl |

## 3.4. SYNTHESIS AND CHARACTERIZATION PAA-COATED UCNP

10.58 mg of UCNP was dissolved in 1 ml of chloroform. Apart from this, 15.8 mg of PAA was dissolved with 2 ml of pure ethanol. When the solution became transparent, UCNPs were added dropwise to the solution. It was stirred at room temperature for 1 day. On the 2nd day, washing was done with ethanol 3 times at 12.000 rpm. (750 µl solution – washed with 750 µl ethanol.)

The characterization of PAA bound to the surface of the particles was determined by FT-IR. Purely synthesized UCNPs and PAA-coated UCNPs were characterized and analyzed. The morphology of UCNPs and PAA-coated UCNPs was determined by TEM. Purely synthesized UCNPs and dopamine coated UCNPs were characterized and analyzed.

Table 3.4.1. Calculations of materials used in PAA coating

| Chemicals | eq | Mwt (g/mol) | n(mmol) | Amount (mg) | Volume/ ml |
|---|---|---|---|---|---|
| PAA | 1.00 | 1800.00 | 114 | 15.8 | |
| UCNP | 0.6 | | | 10.58 | |
| Chloroform | | | | | 1 ml |
| Ethanol | | | | | 2 ml |

## 3.5. SYNTHESIS AND CHARACTERIZATION OF ANTIBODY-CONJUGATED DOPAMIN COATED UCNP

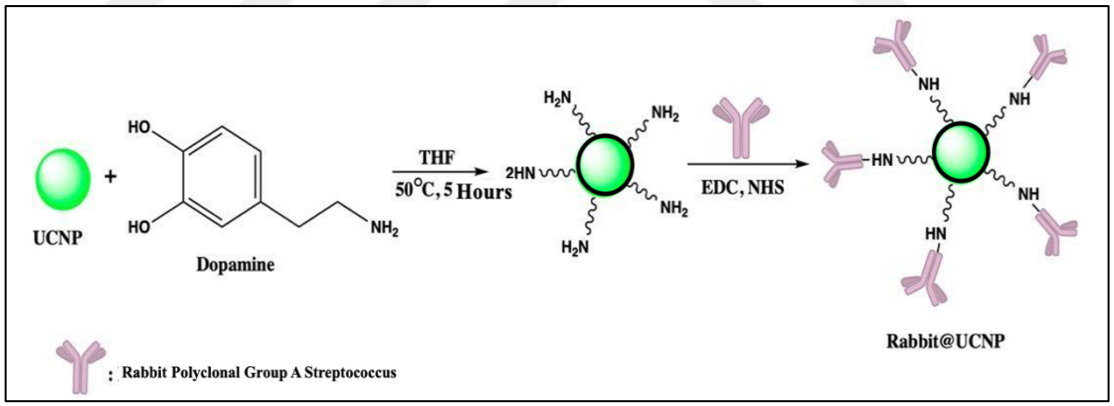


Figure 3.5.1 Conjugation of the surface of dopamine coated UCNP nanoparticles with biomolecules.

Rabbit polyclonal streptococcus group A antibody (Anti-CAS9) specific for streptococcus bacteria was attached to the UCNP + Dopamine coated sample.

Conjugation was carried out by NHS + EDC reaction. Antibodies were incubated with 0.05 M NHS (230 µl) + 0.1 M EDC (1550 µl) for 30 minutes. After completion, dopamine coated UCNPs were added to this solution and mixed for 2 hours at room temperature. DLS for size analysis in conjugation analysis, Zeta-Sizer for determination of surface charges,

characterization of antibodies bound to the surface of particles were determined by FT-IR. Finally, its morphology was analyzed by TEM.

Table 3.5.1. Calculations of materials used in conjugation 1

| Chemicals | eq | Mwt (g/mol) | Amount (mg) | Volume/ml |
|---|---|---|---|---|
| NHS | 0.7 | 115.09 | 11.509 | 230 µl |
| EDC | 1 | 155.25 | 15.52 | 1552 µl |
| Antibody | | | 20 | |

## 3.6. SYNTHESIS AND CHARACTERIZATION OF ANTIBODY-CONJUGATED PAA-COATED UCNP

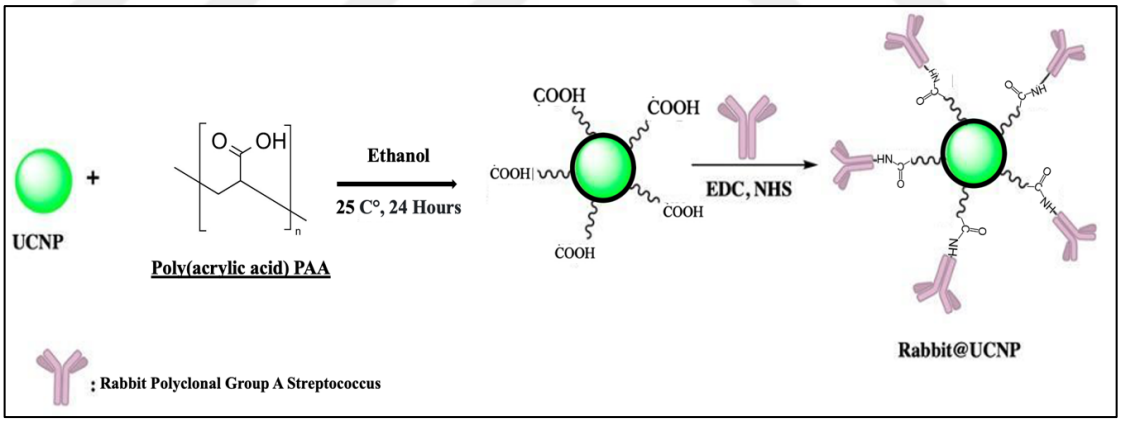


Figure 3.6.1 Conjugation of the surface of PAA-coated UCNP nanoparticles with biomolecules.

Rabbit polyclonal streptococcus group A antibody (Anti-CAS9) specific for streptococcus bacteria was attached to the UCNP @ PAA coated sample. Conjugation was carried out by NHS + EDC reaction. Antibodies were incubated with 0.05 M NHS (230 µl) + 0.1 M EDC (1552 µl) for 30 minutes. After completion, PAA-coated UCNPs were added to this solution and stirred at room temperature for 2 hours. DLS for size analysis in conjugation analysis, Zeta-Sizer for determination of surface charges, characterization of antibodies bound to the

surface of particles were determined by FT-IR. Finally, its morphology was analyzed by TEM.

Table 3.6.1. Calculations of materials used in conjugation 2

| Chemicals | eq | Mwt (g/mol) | Amount (mg) | Volume/ml |
|---|---|---|---|---|
| NHS | 0.7 | 115.09 | 11.509 | 230 µl |
| EDC | 1 | 155.25 | 15.52 | 1552 µl |
| Antibody | | | 20 | |

## 3.7. BACTERIAL GROWTH

Synthetic bacteria, also known as engineered bacteria or synthetic organisms, refer to microorganisms that have been created or modified in the laboratory through synthetic biology techniques. It's important synthetic bacteria are created and used under controlled laboratory conditions, and their release into the environment is subject to strict regulations. Careful risk assessment and containment measures are necessary to prevent unintended consequences and to ensure the responsible use of synthetic organisms.

Streptococcus pyogenes strain is stored in 1.5 ml cryo tubes together with glycerol (20%, v/v) in a nitrogen tank at -80 °C. In order to grow the bacteria, 3 replicates were plated on Tryptone Soy Agar (TSA, Oxoid CM0131B) medium. It was incubated at 37°C for 48 hours. Bacteria growing on the plates were dissolved in 10 ml sterile 0.9% (w/v) NaCl and their density was adjusted to 1.0 in the McFarland device, using a densitometer (Biosan, Latvia), respectively. (± 50 cells/ml).

Saline water (0.85-0.90% NaCl), which is generally used as a dilution solution, is isotonic, meaning that its osmotic pressure is equivalent to the osmotic pressure of microorganisms. For serial dilution, i.e. measurement based on the concentration of bacteria, 9 ml of saline was added to the test tubes. First, a sample of blood agar was taken and added to a glass tube containing 9 ml of saline with a sterile cotton swab. The tube was vortexed for homogeneous distribution of bacteria. When measured on the densimeter, the highest bacterial

concentration was fixed at $10^8$, i.e. 0.5. Then 1 ml of the liquid with the highest concentration was withdrawn and added to the other glass tube. Thus, a value of $10^7$ was obtained and serial dilution was performed depending on the bacterial concentrations. This process was repeated 6 times.

Before starting the test, a cotton swab collected from GAS was dipped into a solution containing 200 µL of 2 M sodium nitrate (425 µl) and 0.027 M citric acid (14 µl), and after waiting for 5 minutes, the solution containing 110 µL of GAS was dropped on the sample pad for test application. Thus, carbohydrate antigens were removed from the environment.

Optimum bacterial density concentration was found by measuring with a densiometer. A concentration of $10^5$ bacteria was used.

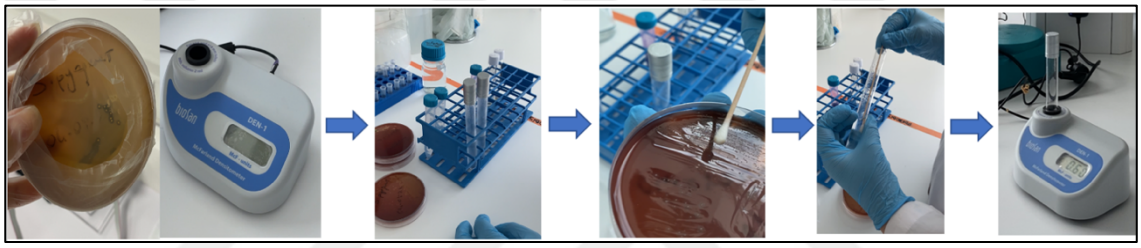

Figure 3.7.1. Measurement of Streptococcus samples by Densimeter

## 3.8. STRIP DESIGN USING THE LATERAL FLOW METHOD

In the setup where the components in the traditional lateral flow method are included, various parameters are analyzed depending on the materials, sizes and concentrations of the components, and the optimum strip design suitable for the coated conjugation design studied has been developed. The concentrations of antibodies applied to the control and test lines on the nitrocellulose membrane, the efficiency of the nitrocellulose membrane Pore Size Dependent Exchange, the distribution speed and the number of repetitions of the lines drawn on the nitrocellulose Membrane on the device, and finally the sensitivity and capillary flow direction of the designed test, increasing the surface tension, viscosity, and static repulsion. The materials and concentrations of the buffer solutions applied to the sample pad, the conjugation pad, and the nitrocellulose membrane have been the parameters used to improve the strip design.

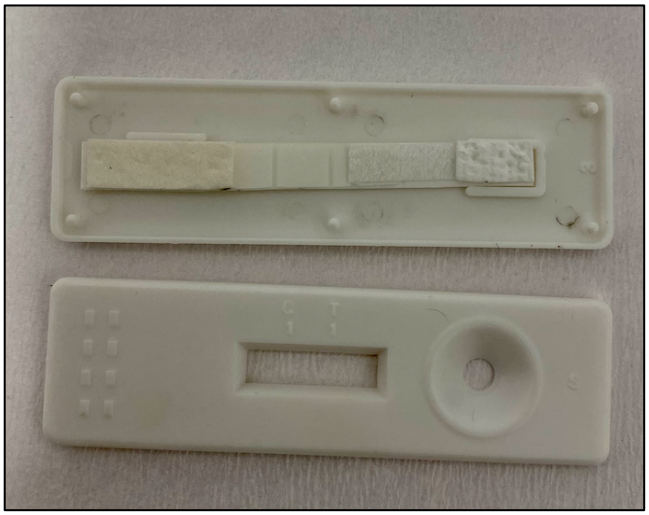

Figure 3.8.1. An example of a strip design placed in a cabinet

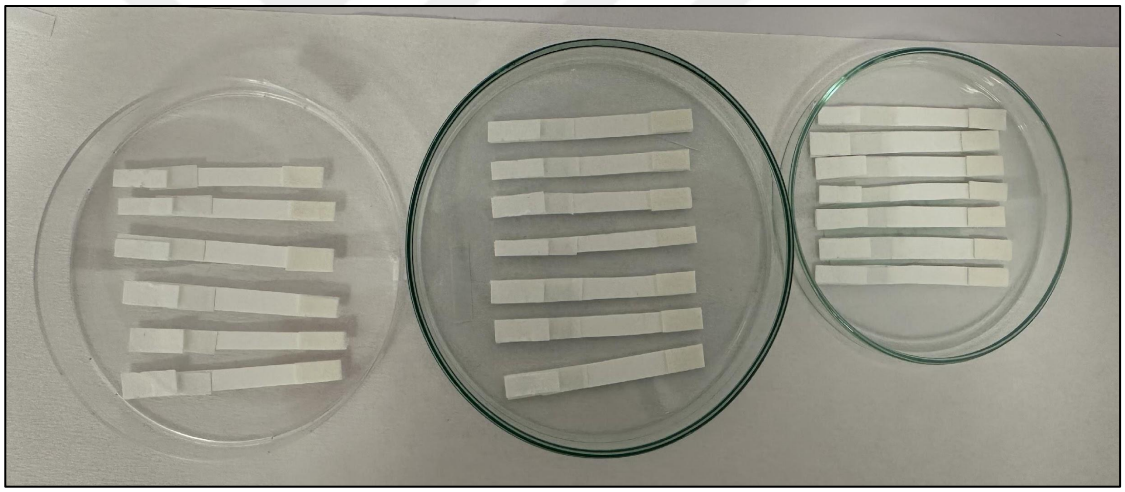

Figure 3.8.2. Examples of replicated strip designs


Figure 3.8.3 Examples of positive and negative strip designs

### 3.8.1. Sample Pad

In lateral flow systems, the sample dropped on the sample pad is loaded at the beginning of the test. It is to ensure the uniform flow and standardization of the buffer conditions of the sample. According to their thickness, 2 different sample pads were used. The codes of the pads are GFB – R7L (0.6) with 0.6 mm thickness and GFB – R7L (0.35) with 0.35 mm thickness, respectively. Firstly, the bed volume was calculated on the sample pad. The formula used for bed volume; Bed volume = Total volume of pad* Porosity (%). Calculations were made according to the length, width, thickness and porosity of the sample pads. Length - 1 cm, Width - 0.5 cm, Thickness - 0.6 cm, Porosity - 70% - 0.7 = 0.021 cm3 = 21µl. The same calculation was calculated for the 0.35 mm thick sample pad and the buffer solutions were used. While preparing the buffer solutions of the sample pad, tween 20 as detergent, bovine serum albumin (BSA) as blocking agents and as a preservative buffer solution were dried at 37°C for 2 hours and vacuumed at 0.2 bar pressure for 1 hour. A PBS solution containing 0.5% BSA and 0.05% Tween 20 was prepared. It should be stored at 4°C until needed.

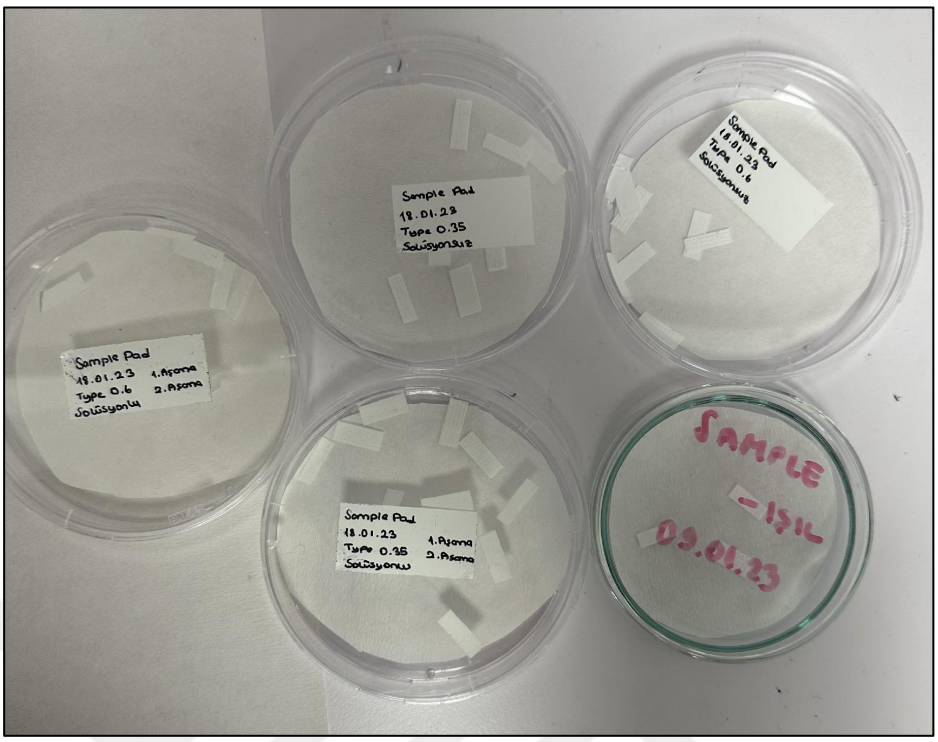


Figure 3.8.1.1. Sample pads prepared in different parameters.

### 3.8.2. Conjugation Pad

They are conjugated nanoparticles dried for fixation, then wetted by the sample, and finally achieving initial interaction is the key between the labeled bioreceptor and the target. 2 different conjugation pads were used. These; They are pads coded PT-R5 with minimal additives in their pores and PT-R7 containing buffers for uniform movement of gold, for example.

In the buffer solution preparation of the conjugate pad, borate buffer was used as buffering agents, sucrose as stabilizing and solubilization reagent, BSA as blocking agent and tween 20 as detergents. After adding nanoparticle and antibody conjugate, it was dried at 37°C for 2 hours and vacuumed at 0.2 bar pressure for 1 hour. PBS solution containing 5% sucrose, 1% BSA, 0.5% Tween 20 should be stored at 4°C. Essential for the release and flow efficiency of the Sucrose and Tween 20 conjugated nanoparticle solution. After these procedures, 10 µl of antibody conjugation solution was added and dried under room conditions.

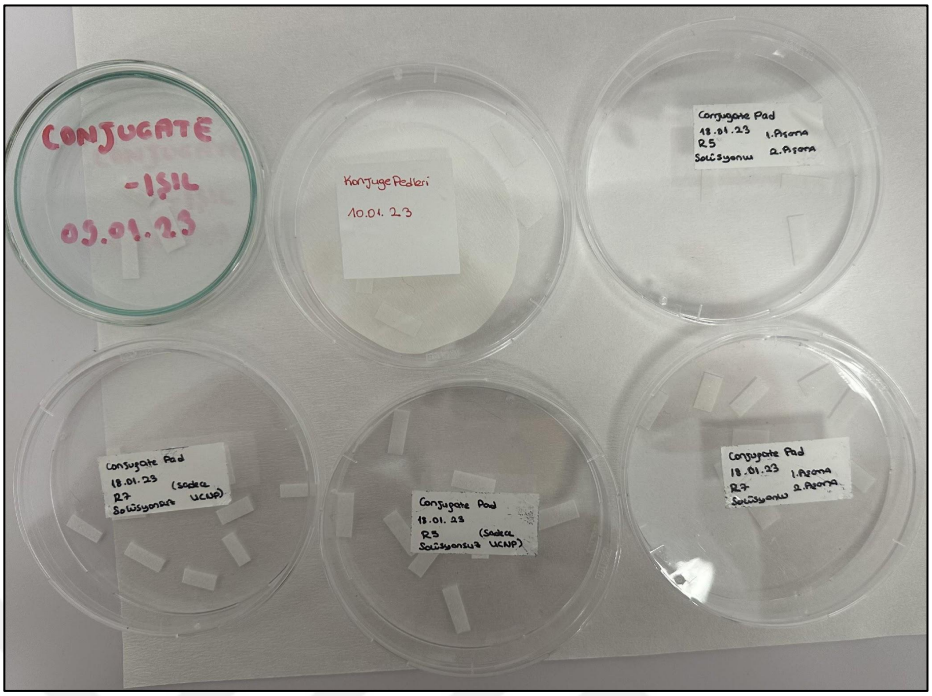


Figure 3.8.2.1. Conjugation pads prepared in different parameters.


Figure 3.8.2.2. Incubation of conjugation pads prepared in different parameters.

### 3.8.3. Membrane

The main features of the membrane are that firstly it facilitates a homogeneous flow, secondly it provides a solid functionalization to capture the bioreceptor and shows low non-

specific binding. The use of nitrocellulose material in the membrane, the binding of the antibody increased the flow efficiency. Capillary flow direction based on pore size was roughly calculated as 135 seconds based on 8 microns. However, in the strip design, 4 different membrane types were used according to the pore sizes.

Buffering agents, ammonium acetate or phosphate buffer should be used to promote membrane binding. For this reason, ammonium phosphate was used. As stabilizing and solubilizing reagents, 0.1% lactose or 1% trehalose may be included to help stabilize the capture bioreceptor after the membrane has dried. However, lactose or trehalose was not used because there was no homogeneous distribution on the membrane after inclusion. 1% - 10% ethanol was used to reduce surface tension, viscosity and static repulsion. Finally, the membrane was immersed in 2% BSA, 0.01 M PBS for 20 minutes. At the end of the period, the membrane was immersed in a wash buffer 0.05% SDS pH 7.4 and 0.005 M PBS with gentle shaking for 15 minutes [54]. This process, repeated twice, was dried at 37°C for 2 hours. In this process, it is very important to remove BSA from the membrane. If not removed, it may cover part of the drawn lines.

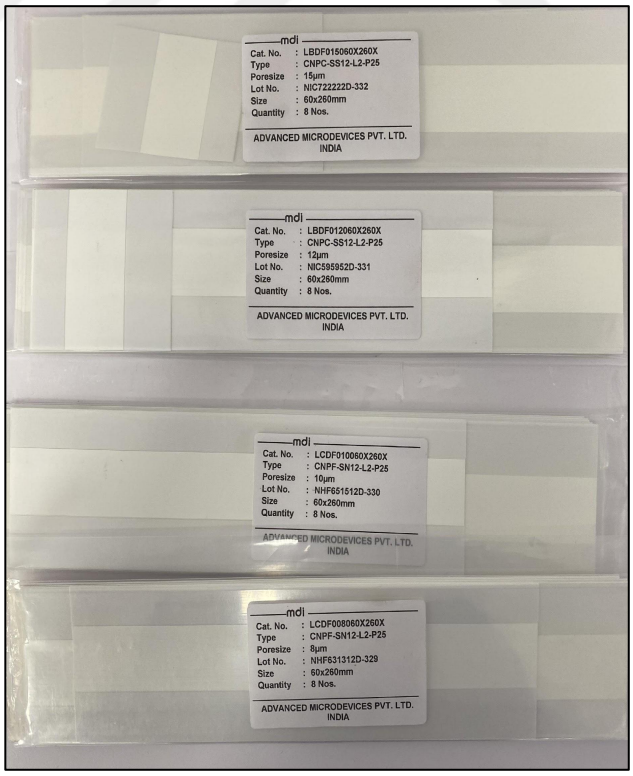


Figure 3.8.3.1 Nitrocellulose membranes with different pore sizes

**Product** Nitrocellulose Membrane for Rapid Test

**Product Type** CNPF

**Composition**

| Constituent | Material | Pore Size | | |
|---|---|---|---|---|
| | | 5 µm | 8 µm | 10 µm |
| Polymer | Nitrocellulose | Yes | Yes | Yes |
| Backing | Transparent Polyester | Yes | Yes | Yes |

**Physical Properties**

| Property | Pore Size | | |
|---|---|---|---|
| | 5 µm | 8 µm | 10 µm |
| Appearance: White film on a transparent backing | Yes | Yes | Yes |
| Thickness of backing (microns) | 102 ± 5 | 102 ± 5 | 102 ± 5 |
| Thickness of membrane (microns) | 100 ± 15 | 110 ± 15 | 100 ± 15 |

**Membrane Performance Characteristics**

| Characteristics | Pore sizes | | |
|---|---|---|---|
| | 5 µm | 8 µm | 10 µm |
| Mean wicking time (seconds) (4cm distance, Normal Saline) | 220 ± 25 | 170 ± 25 | 125 ± 25 |
| Protein Binding (µg/cm$^2$) | ≥ 35 | ≥ 33 | ≥ 30 |

Figure 3.8.3.2 Membranes Product Information

Table 3.8.3.1. Membrane models

| Cat. No. | Pore Size |
|---|---|
| CNPF – SNI2 | 8 micrometer |
| CNPF – SNI2 | 10 micrometer |
| CNPF – SNI2 | 12 micrometer |
| CNPF – SNI2 | 15 micrometer |

Figure 3.8.3.4. Membrane obtained with trehalose solution.

### 3.8.4. Drawing of Antibodies with the Device on the Membrane

The drawing was made with the device designed at Yeditepe University. In this device using the Arduino software base, 200 µl of 1 mg/ml solutions of antibodies were prepared and drawn on the membrane as test and control lines. Using a distribution rate of 0.5 ml/cm, a speed of 50 mm/sec, 20 µl was sufficient to prepare a 30 cm nitrocellulose membrane. It was then dried at 37°C for 2 hours. Different from the antibody conjugated to UCNPs for the sandwich assay test in the designed strip, anti-donkey antibody was used on the test line and donkey anti-rabbit antibody was used on the control line to bind to 2 different epitopes, which is specific to the Anti-Cas9 antibody. In addition, 3 different concentrations of antibodies applied to the control and test lines on the Nitrocellulose Membrane were determined. Depending on the efficiency of these concentrations, the optimum concentration was analyzed and selected in a fluorescence spectrophotometer.

Table 3.8.4.1. Concentrations of antibodies

| | **Test line Anti Donkey** | **Control line Donkey Anti Rabbit** |
|---|---|---|
| 1. Antibody concentration | 5 mg - 200 µl PBS | 10.2µl - 200 µl PBS |
| 2. Antibody concentration | 10 mg - 200 µl PBS | 15. 4 µl - 200 µl PBS |
| 3. Antibody concentration | 15 mg - 200 µl PBS | 30.8 µl - 200 µl PBS |

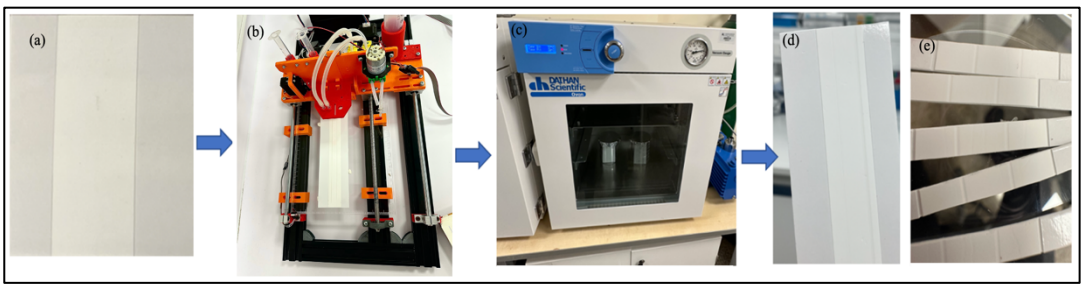


Figure 3.8.4.1. (a) Backing card and nitrocellulose membran, (b) Test and control line drawing on the device, (c) Incubation of membranes at 37°C after antibody drawing, (d) nitrosellulose membran after incubation, (e) Membranes that are ready for testing with manual cutting after incubation.

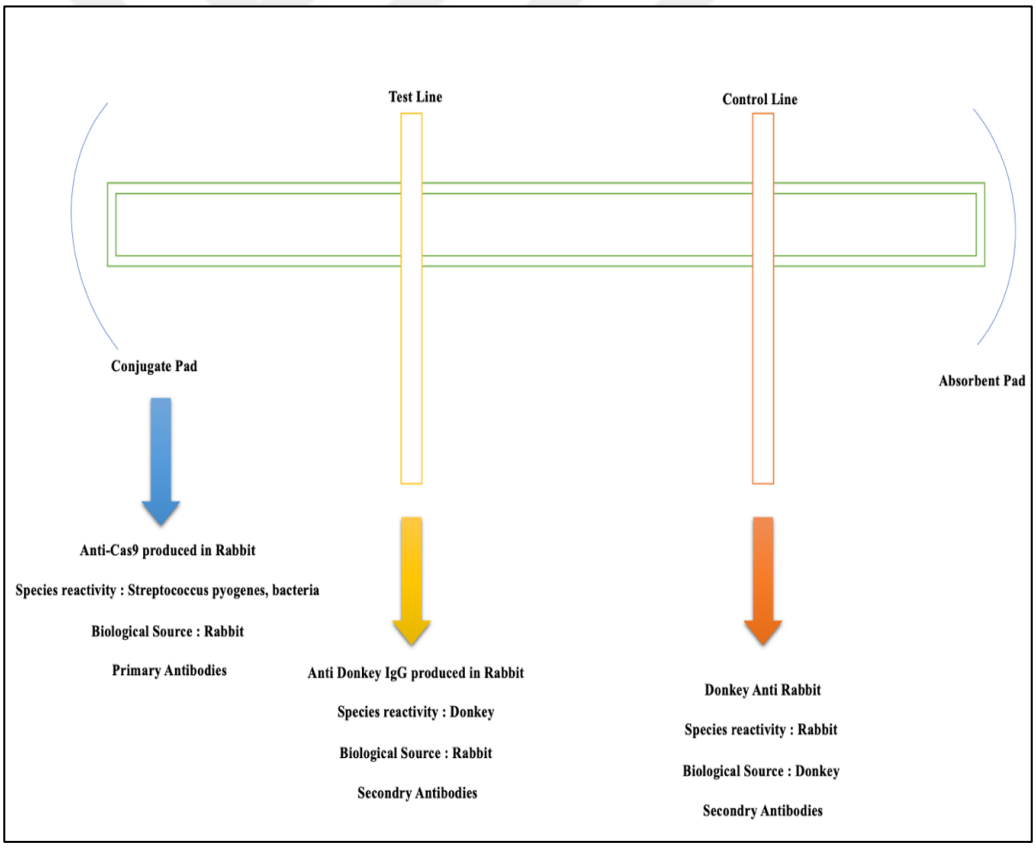


Figure 3.8.4.6. Antibody materials used in conjugate pad, test, and control lines [6,55].

### 3.8.5. Absorbent Pad

Used to control the sample volume a strip can hold. In the absence of the absorbent pad, when the liquid reaches the end of the membrane, the flow stops, and the liquid evaporates uniformly along the strip. AQ305892D absorbent pad was used. Buffer solution was not applied to the absorbent pad.

# 4. RESULTS AND DISCUSSION

In this section, the overall findings of the study will be described. In short, the characterizations of the coating and conjugating of nanoparticles, and the components of the lateral flow assay strips will be given.

## 4.1. MORPHOLOGICAL AND STRUCTURAL CHARACTERIZATIONS

### 4.1.1. SEM & TEM

The morphology and size distribution of NaYF4:Yb, Er (UCNP) sample was studied by Scanning electron microscope (SEM) and Transmission Electron Microscope in figure 4.1.1.1 and 4.1.1.2 (a).

Both SEM and TEM observations showed that particles were spherical, and their size were measured to be ~26 nm. Histograms of particle size distribution were determined by imaging software (Image J) is shown in figure 4.1.1.2(b).

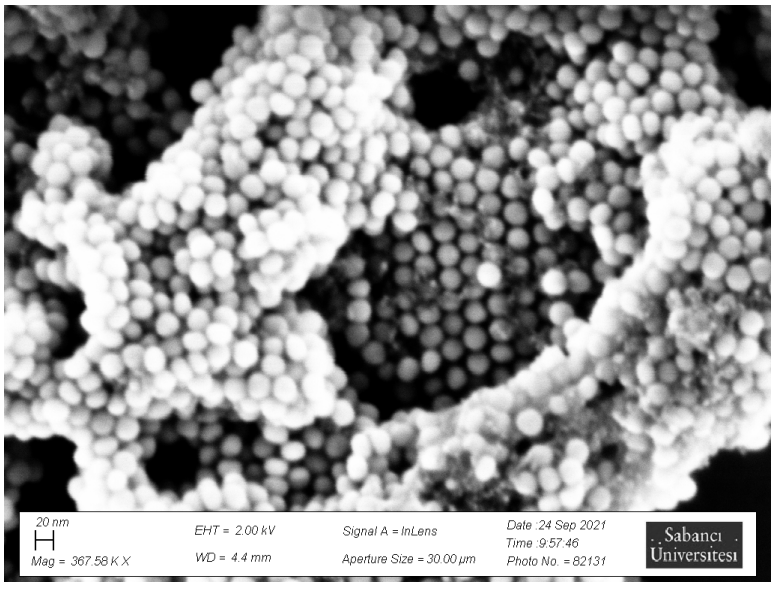


Figure 4.1.1.1. SEM image of NaYF4:Yb, Er nanoparticles

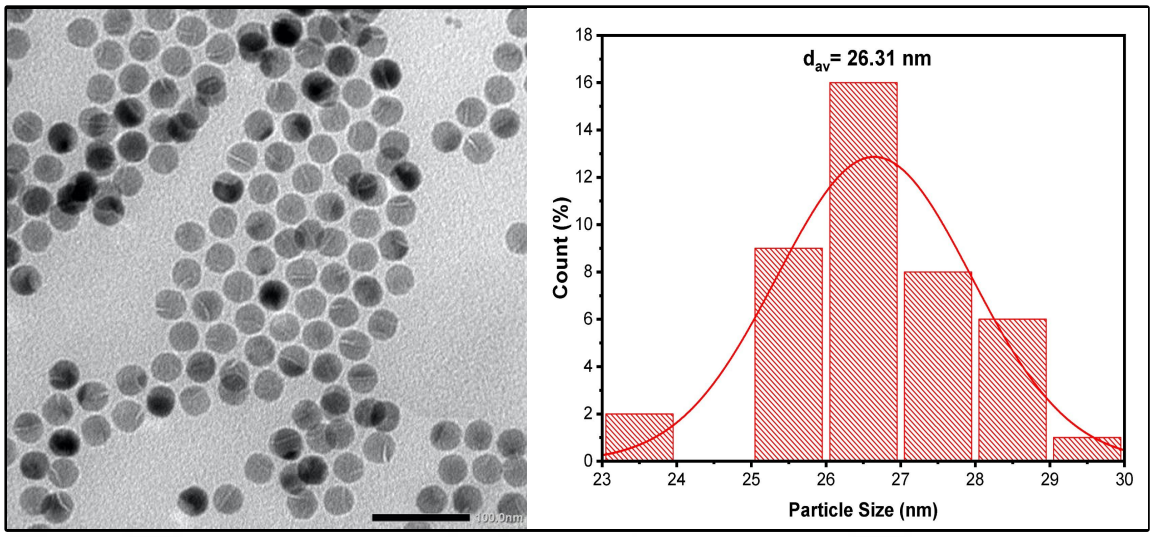


Figure 4.1.1.2. (a) TEM image of NaYF4 nanoparticles, (b) histograms of particle size distribution.

High resolution TEM (HRTEM) image of UCNP nanoparticles (Fig4.1.1.3) presents a uniform lattice fringe with d-spacing of 0.52 nm that is compatible with hexagonal phase NaYF4.

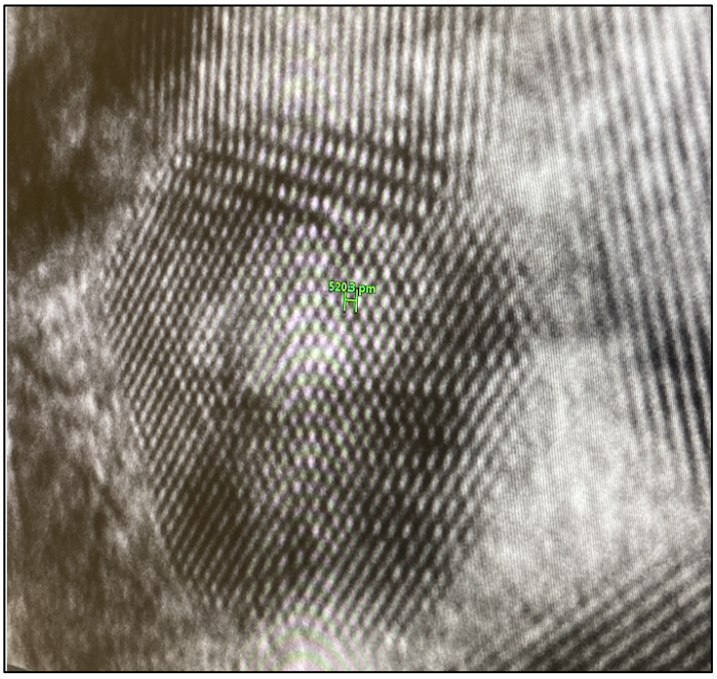

Figure 4.1.1.3. HRTEM image of NaYF4: Yb, Er nanoparticles

UCNPs have hydrophobic ligands (carbonyl groups) on their surface after synthesis, so the surface has been modified by ligand exchange to make it hydrophilic. In order to make the surface hydrophilic, UCNPs' surfaces were covered with both Dopamine and PAA molecules individually. Figure 4.1.1.4 presents TEM images of UCNPs after Dopamine coating. Figure 4.1.1.5 presents TEM images of UCNPs after PAA coating. Although Dopamine is a small molecule compared to the PAA, after Dopamine coating each particle size was increased to 150-200 nm. This may have been caused by agglomeration of dopamine as a result of its high concentration. However, nanoparticles coated with PAA demonstrate a small increment in particle size.

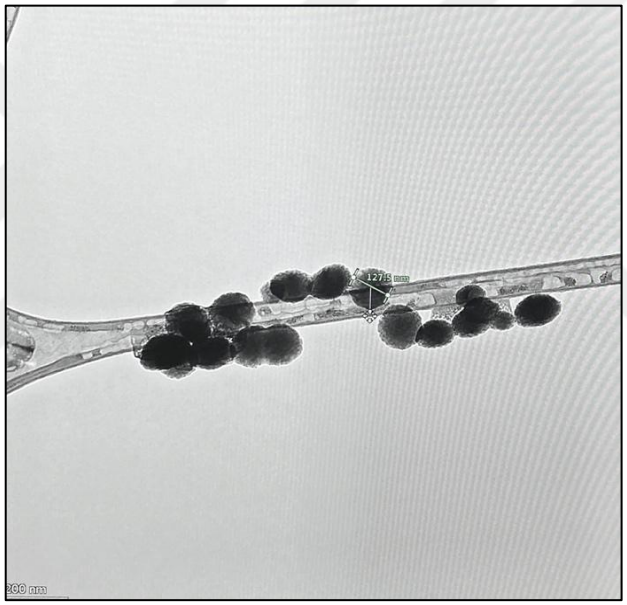

Figure 4.1.1.4. TEM images of NaYF4:Yb, Er nanoparticles coated with dopamine

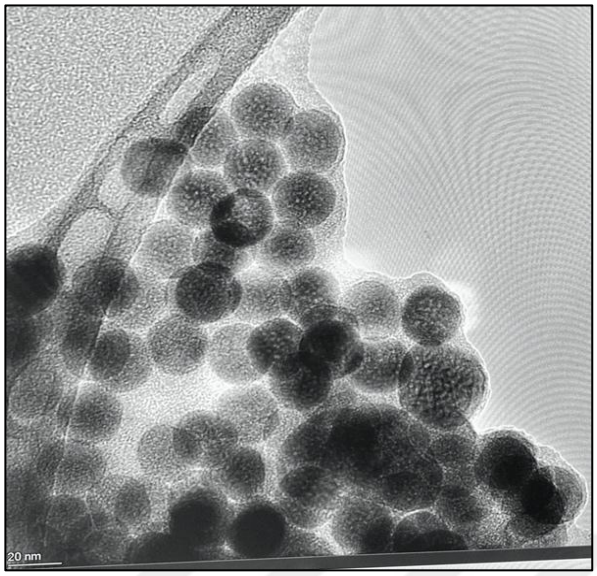


Figure 4.1.1.5. TEM images of $NaYF_4$:Yb, Er nanoparticles coated with PAA

### 4.1.2. Structural Analysis with XRD

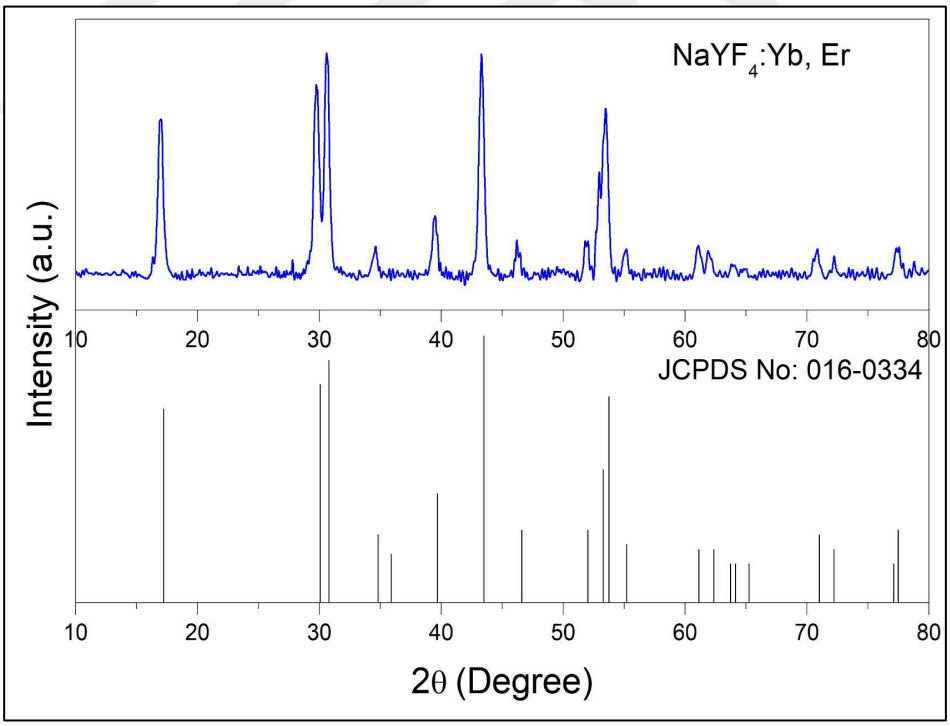


Figure 4.1.2.1. XRD Pattern of NaYF4:Yb, Er

The peaks in the XRD pattern match well with those in the beta (hexagonal) phase indexed with JCPDS card number 016-0334 shown in figure 4.1.2.1. As a result of processing the

XRD pattern in Scherrer equations, the particle size was found to be ~20 nm, which is consistent with the TEM analysis.

## 4.2. SPECTROSCOPIC CHARACTERIZATIONS

### 4.2.1. DLS & Zeta Potential

The size analysis of the particles obtained will be determined by DLS and the changes in polydispersity (PDI) were also followed. Processing the XRD pattern in Scherrer equations, the particle size was found to be ~20 nm, which is consistent with the TEM analysis. According to DLS results, the particle size was found to be 646.1 nm before dopamine coating and their size was increased to 743.9 nm after dopamine coating and for the PAA coated nanoparticle the size observed in 998.1 nm. Although these results also support the increment in particle size due to dopamine and PAA coating where the findings are not compatible with neither TEM nor XRD.

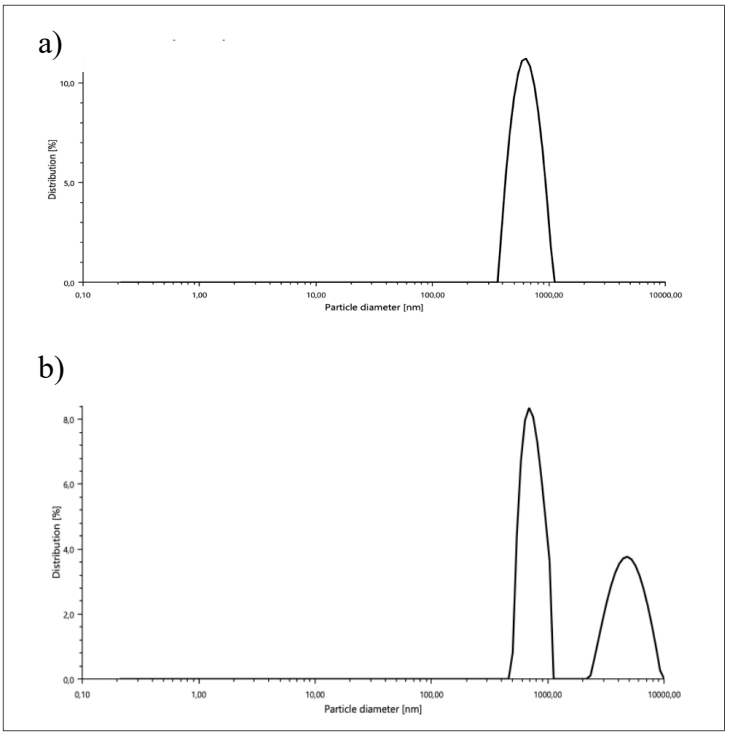


Figure 4.2.1.1. (a) Particle size distribution by intensity UCNP-dopamin. (b) Particle size distribution by intensity UCNP-dopamin-antibody conjugation.

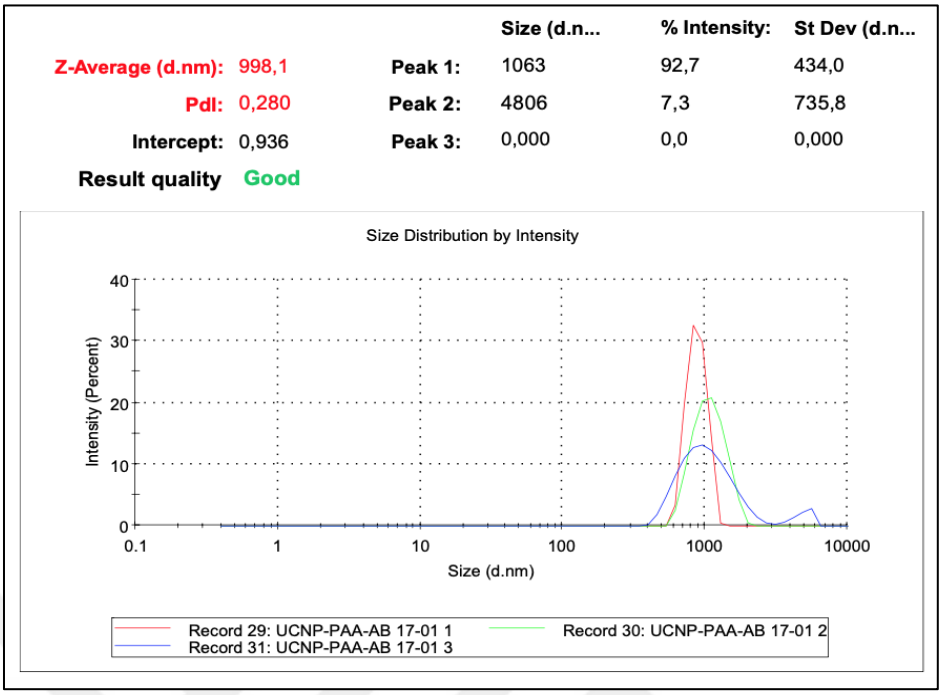


Figure 4.2.1.2. Particle size distribution by intensity UCNP-PAA-AB.

The determination of the surface charges of UCNPs and antibody was used to zetasizer. Figure 4.2.1.3 a), shows the zeta potential of the UCNPs at 7.77 mV. The zeta potential of the UCNP-Dopamin conjugate was measured as -3.73 mV in figure. 4.2.1.3 b). After adding to dopamin and conjugating the antibody, negatively charged O-H groups of the dopamin caused surface potential to negatively shift, indicating a successful conjugation. After addition of the antibody, the zeta potential was quantified as -10.7 in figure 4.2.1.3 c).

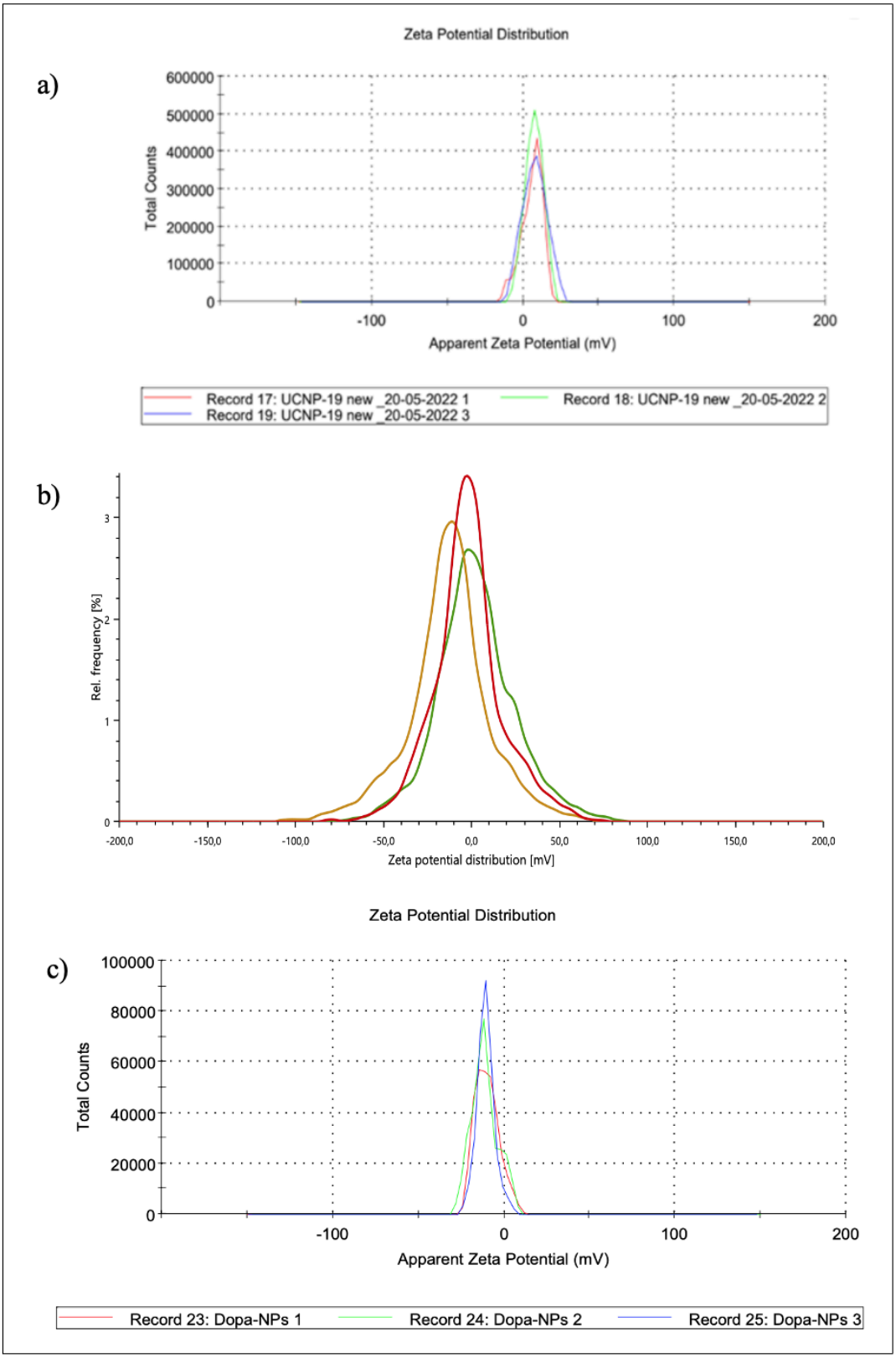


Figure 4.2.1.3. Zeta potential distribution of the; (a) Pure UCNP, (b) Surface modified UCNP with dopamin (c) Antibody conjugated UCNP-Dopamin.

The determination of the surface charges of UCNPs and antibody was used to zetasizer. Figure 4.2.1.4 a), shows the zeta potential of the UCNPs at 7.77 mV. The zeta potential of the UCNP-PAA conjugate was measured as -37.0 mV in figure. 4.2.1.4 b). After adding to PAA and conjugating the antibody, negatively charged carboxylic groups of the PAA caused surface potential to negatively shift, indicating a successful conjugation. After addition of the antibody, the zeta potential was quantified as -33.2 in figure 4.2.1.4 c). Due to amine groups of the antibody, surface potential was positively shifted, as it was expected to be occurred.

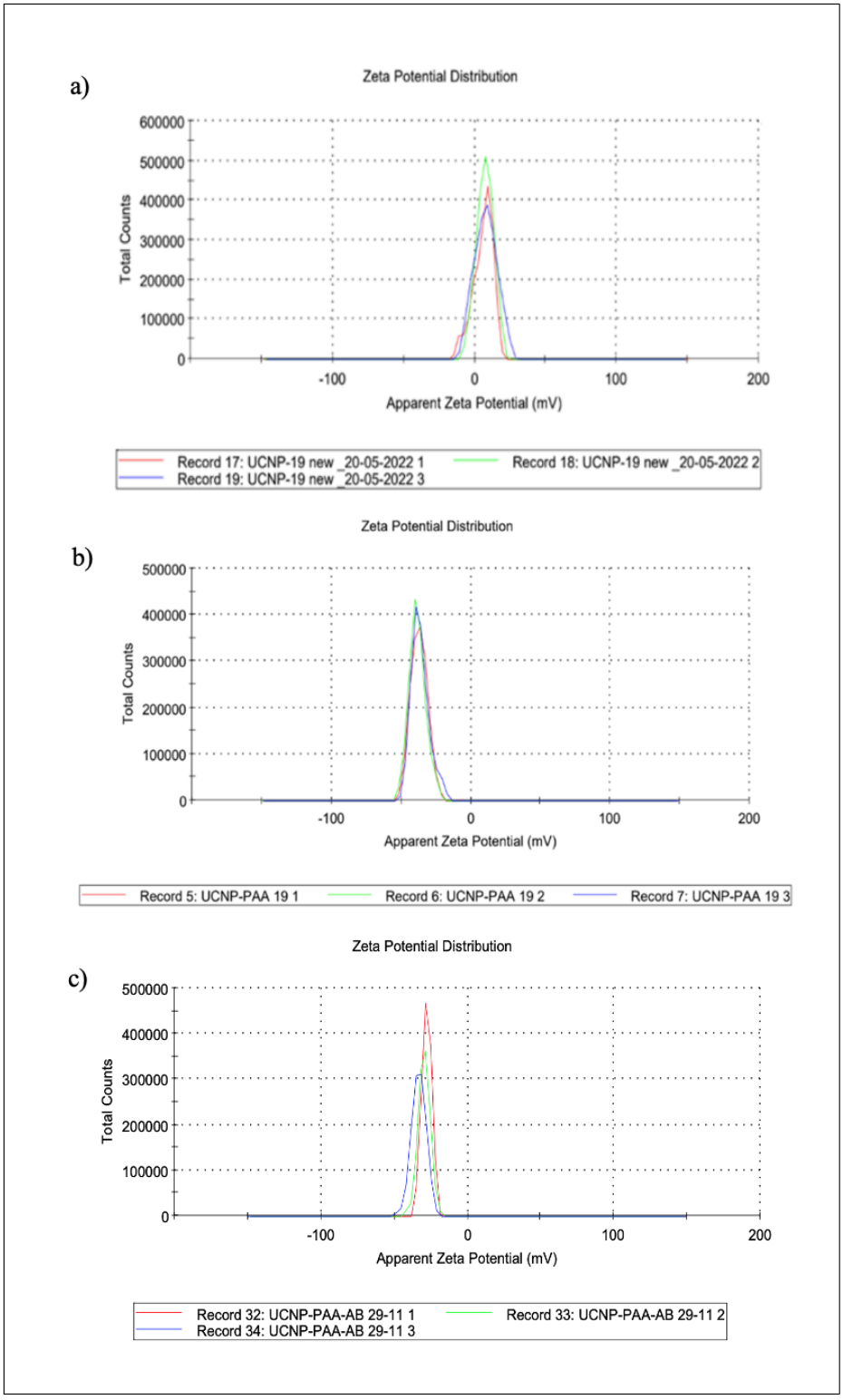


Figure 4.2.1.4. Zeta potential distribution of the; (a) Pure UCNP, (b) Surface modified UCNP with PAA (c) Antibody conjugated UCNP.

### 4.2.2. UV-VIS

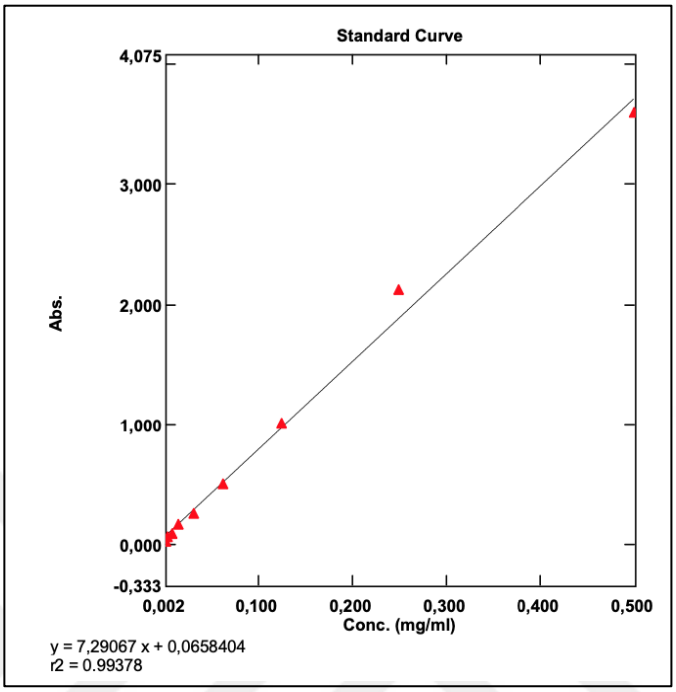


Figure 4.2.2.1. Uv-vis spectroscopy analysis standart curve with PBS

Table 4.2.2.1. Uv-vis spectroscopy analysis results

.....
Standard Table

| | Sample ID | Type | Ex | Conc | WL284,0 | Wgt.Factor | Comments |
|---|---|---|---|---|---|---|---|
| 1 | 10 | Standard | | 0.002 | 0.035 | 1.000 | |
| 2 | 9 | Standard | | 0.004 | 0.071 | 1.000 | |
| 3 | 8 | Standard | | 0.008 | 0.097 | 1.000 | |
| 4 | 7 | Standard | | 0.016 | 0.169 | 1.000 | |
| 5 | 6 | Standard | | 0.031 | 0.262 | 1.000 | |
| 6 | 5 | Standard | | 0.063 | 0.511 | 1.000 | |
| 7 | 4 | Standard | | 0.125 | 1.014 | 1.000 | |
| 8 | 3 | Standard | | 0.250 | 2.120 | 1.000 | |
| 9 | 2 | Standard | | 0.500 | 3.591 | 1.000 | |

Sample Table

| | Sample ID | Type | Ex | Conc | WL284,0 | Comments |
|---|---|---|---|---|---|---|
| 1 | Dopaminucnp | Unknown | | 0.510 | 3.783 | |
| 2 | | | | | | |

Standard Table

| | Sample ID | Type | Ex | Conc | WL284,0 | Wgt.Factor | Comments |
|---|---|---|---|---|---|---|---|
| 10 | 1 | Standard | ✔ | 1.000 | 3.751 | 1.000 | |
| 11 | | | | | | | |

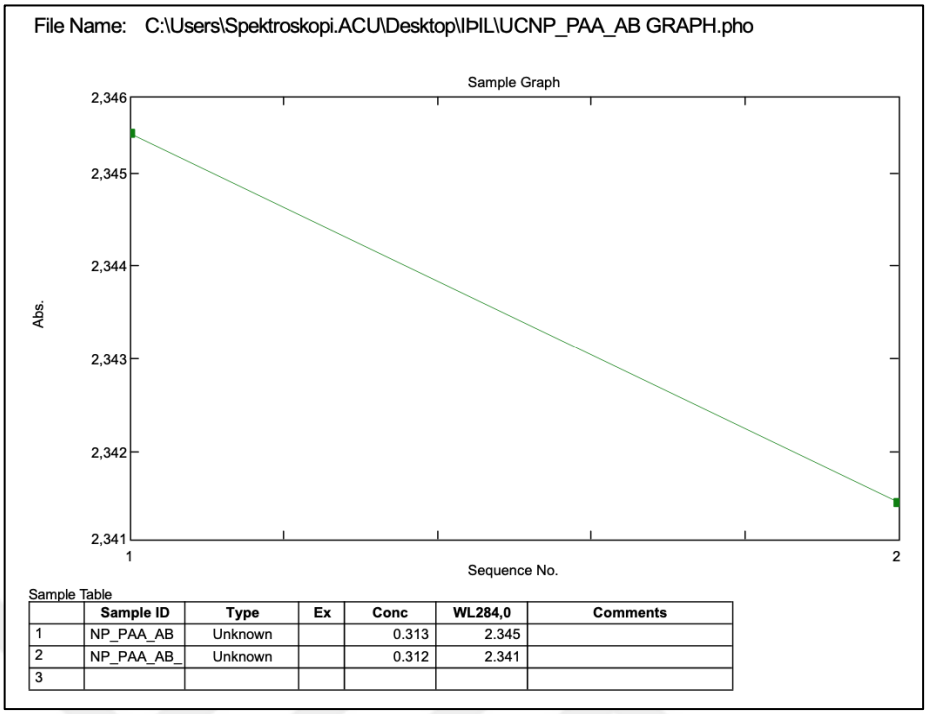


Sample Table

| | Sample ID | Type | Ex | Conc | WL284,0 | Comments |
|---|---|---|---|---|---|---|
| 1 | NP_PAA_AB | Unknown | | 0.313 | 2.345 | |
| 2 | NP_PAA_AB_ | Unknown | | 0.312 | 2.341 | |
| 3 | | | | | | |

Figure 4.2.2.2. Uv-vis spectroscopy analysis sample UCNP-PAA-antibody graph

According to Lambert-Beer's law, the relation of absorbance to concentration is given by,

$$A = \varepsilon 0LC \qquad (1)$$

where A is absorbance (unitless),
ε0 (epsilon) is molar absorption coefficient of the analyte for a certain wavelength ($l \cdot mol^{-1} \cdot cm^{-1}$),
L is path length (cm) through a sample cuvette and
C is the concentration of the analyte ($mol \cdot l^{-1}$).

To find the absorbance value, firstly, the background was taken and samples diluted at 10 different concentrations in PBS, with the UV-Vis Spectrophotometer. The highest absorbance wavelength was chosen in the spectrum. Then, a calibration curve with absorbance at this wavelength was plotted against the different concentration (Fig 4.2.2.1).

By fitting the points with a straight line, concentration values could be determined for a specific absorbance value. From figure 4.2.2.1, the absorbance peak at 323 nm corresponds to the existence of 51% dopamine and 49% nanoparticles in the examined solution.

Moreover, for the case of PAA-coated UCNP, the existence of %31 PAA and %69 nanoparticles detected in the examined solution.

### 4.2.3. FT-IR

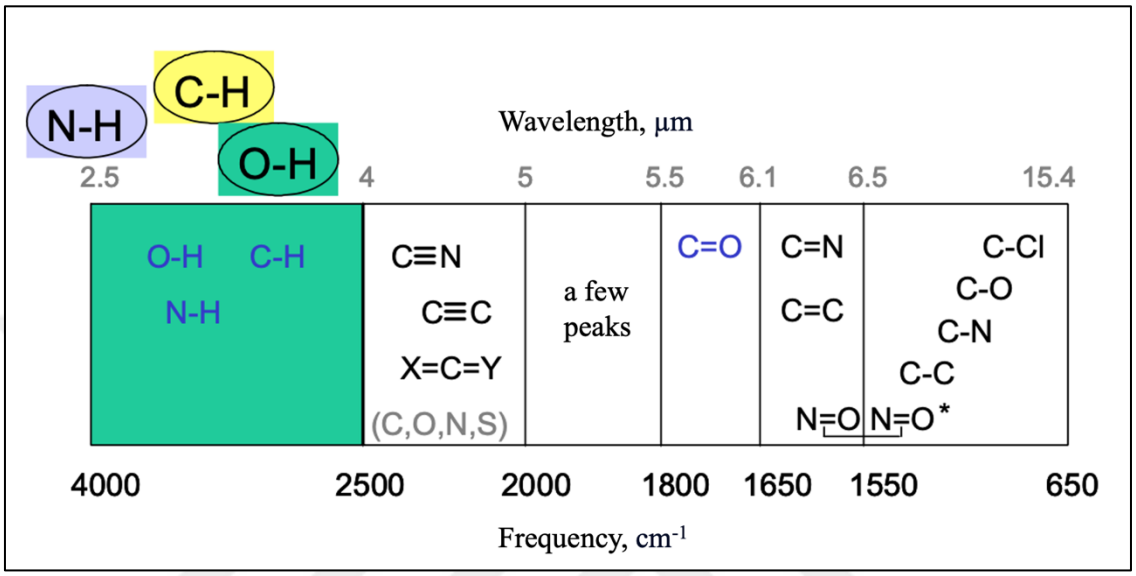


Figure 4.2.3.1. O-H, N-H, C-H stress region; 4000-2500 cm-1

O-H, N-H and C-H bonds are seen in the 4000-2500 cm-1 stretching region. Strong absorption peaks are observed in this region, mostly due to the stretching vibration of the hydrogen atom with other atoms. Since the hydrogen atom is very light compared to another atom to which it is attached, the movement is large; as a result, absorption is not affected by the immobility of the molecule. In addition, the hydrogen stretching frequency being higher than other chemical bonds reduces the interaction of this vibration with other vibrations. O-H and N-H stretching vibrations are defined by the absorption peaks in the same region, that is, in the 3700-3100 cm-1 region. Unlike N-H bonds, peaks belonging to O-H tend to be found in higher wavenumbers.

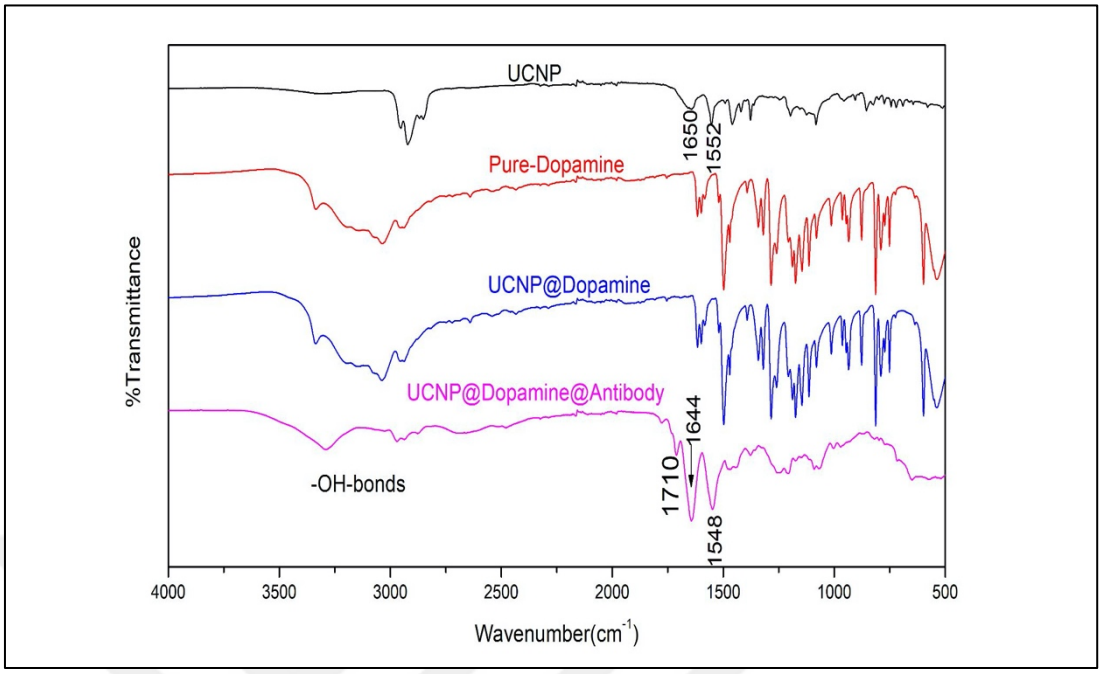


Figure 4.2.3.2. FT-IR analysis of UCNP, dopamine and UCNP-dopamine

The FT-IR spectroscopy based chemical characterization of bare UCNP nanoparticles, Dopamine, Dopamine-UCNP nanoparticles and a streptococcus specific antibody conjugated dopamine-UCNP nanoparticles was done as shown in Figure 4.2.3.2. The peaks between 3700- 3100 $cm^{-1}$ corresponding to stretching vibrations of -OH and N-H groups indicates the conjugation of dopamine with two aromatic hydroxyl groups on the nanoparticle surface. The amine groups of dopamine were covalently linked to carbonyl groups of the antibody, which was understood from the presence of peaks at 1548 $cm^{-1}$, corresponding to the secondary amide protons of antibody. This showed us that the nanoparticles were coated with dopamine and further conjugated to antibody. In addition, there is a peak appearing at 1552 $cm^{-1}$ in the pure nanoparticle spectrum but not in the one for dopamine. This is due to sodium oleic acid from UCNPs because this acid variety also has carbonyl bonds.

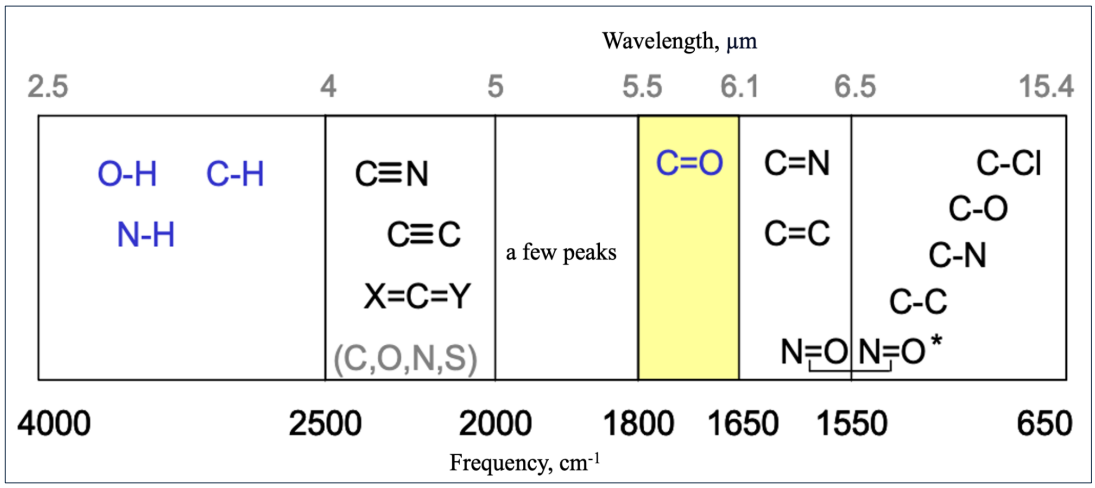


Figure 4.2.3.3. C=O stress region; 1800-1650 cm-1

The Carbonyl Group is C=O as shown in Figure 1; It shows vibrations in the region of 1800-1650 $cm^{-1}$. For example, having carbonyl groups; For aldehydes, acids, amides and carbonates, esters, acid chlorides and acid anhydrides, the flexural vibration is defined and determined by its absorption in this region. C=O, the bond belonging to these groups, are the strongest peaks in the spectrum. This is due to the large C=O dipole moment.

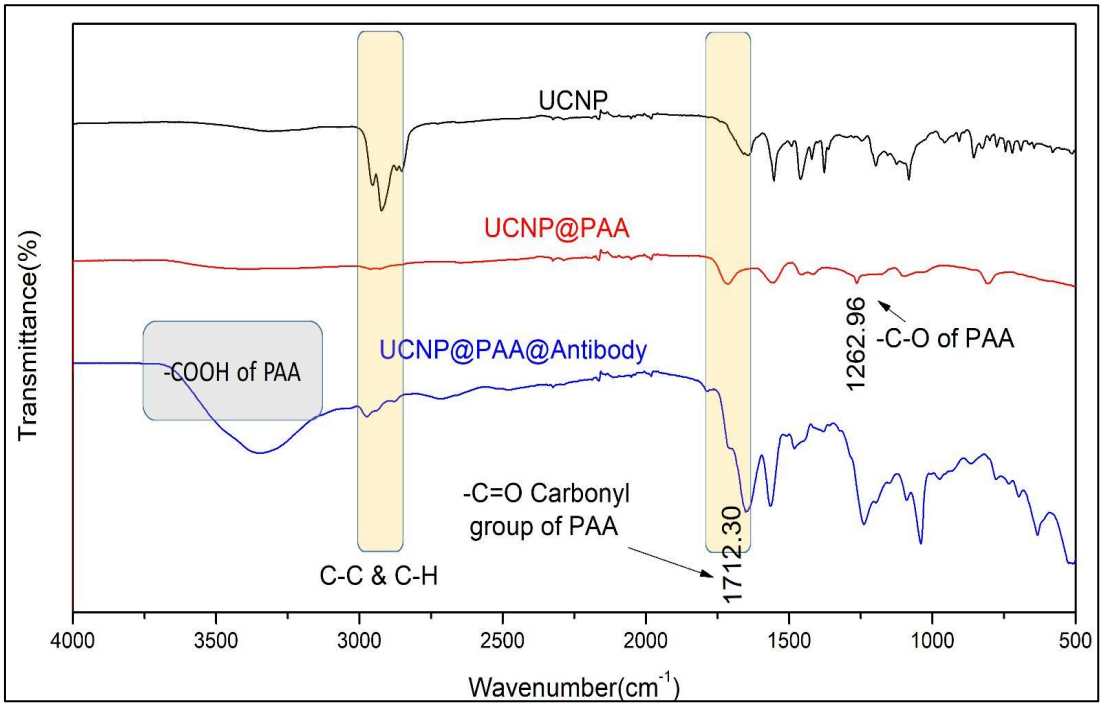


Figure 4.2.3.4. FT-IR analysis of bare UCNP, PAA and UCNP-PAA-AB

The comparison of FT-IR spectra indicates the conjugation of antibodies on UCNP nanoparticles coated with PAA, as given in Figure 4.2.3.4. Upon PAA coating, the carboxylic acid –OH group is observed in the band of approximately 3300 $cm^{-1}$ as a broad peak, as expected. In addition, –C=O stretching peaks in the PAA structure are observed at 1712.3 $cm^{-1}$ and its bending peaks seem to appear at 1064 and 510 $cm^{-1}$, respectively, that marks the successful implementation of the PAA coating. After this step, the amine groups of the selected antibody were covalently linked to the carbonyl groups of PAA by EDC-NHS chemistry through amide bond formation. It can be easily seen in the FT-IR spectrum where antibodies are conjugated on the nanoparticle. The observed amide carbonyl peak at 1641 $cm^{-1}$ indicates that the antibody was conjugated to PAA polymer. In addition, the hydroxyl and amine groups of the chemical structure of the antibody also appear at around 3300 $cm^{-1}$ regions, which now gets broader with the presence of conjugated antibody onto the nanoparticle surface. The –C-O stretching peak at 1006 $cm^{-1}$ and the –C-O bending peak at 650 $cm^{-1}$ belong to the conjugated antibody. Based on these comparisons, both the PAA coating and the antibody conjugation steps were understood to be performed successfully.

### 4.2.4. Photoluminescence Analysis (PL)

The PL spectrum of the NaYF4 :Yb, Er nanoparticles exhibit peaks around 521 nm, 545 nm and 660 nm. The peak pattern obtained from PL characterization matches almost exactly with the emissions reported by Wang. et al. for the NaYF4 :Yb, Er nanoparticles.

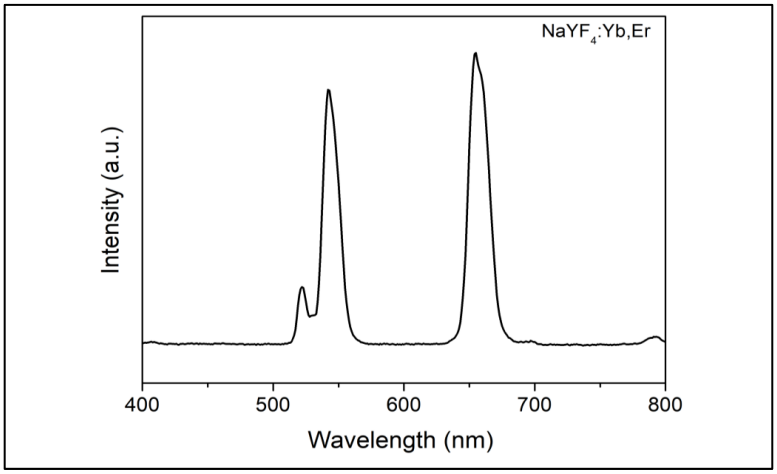


Figure 4.2.4.1. PL spectra of the NaYF4 :Yb, Er nanoparticles. There are three emission peaks which are around 521 nm, 545 nm and 660 nm wavelengths.

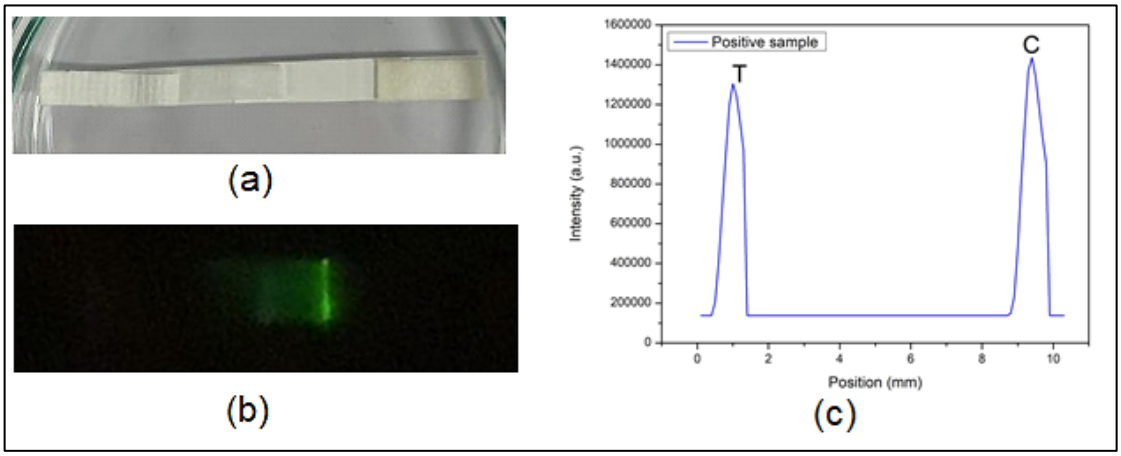


Figure 4.2.4.2. (a) Camera image taken on strip under white light, (b) Camera image under near infrared light, (c) Signals received in spectrophotometer over Test and Control lines.

After the sample containing the analyte was dropped onto the sample pad, camera images were taken at 15., 30. and 45. minutes depending on time. After 30 minutes, the lines started to become clear and clear images were obtained only at the 45th minute.

## 4.3. STRIP CHARACTERIZATION

### 4.3.1. Fluorescent Microscope

Microscope, which enables the visibility of tissue sections under the appropriate wavelength of light of certain fluorescent substances. The samples were stained with previously obtained specific antibodies and the desired lines were visualized. In order to obtain images, dyes that fluoresce when they encounter these rays are used. The fluorescent dyes in this strip design are up-conversion nanoparticles. In fluorescent microscopes, some filters are used to display the wavelength reflection. Images were taken with the FITC filter among four different filters in figure 4.3.1.1 b). The wavelength of this filter has excitation and emission spectrum peak wavelengths in the range of 495-519 nanometers. This filter is typically used for monoclonal antibodies and gives the samples a green color for us to view. Figure 4.3.1.2 Shows the distribution of UCNPs as a sample on the conjugation pad, which was taken from the negative test, conjugated with streptococcus specific anti cas-9. Based on this display,

test and control lines were obtained from the microscope. The presence of UCNPs in these obtained lines indicates that the test performed lateral flow.

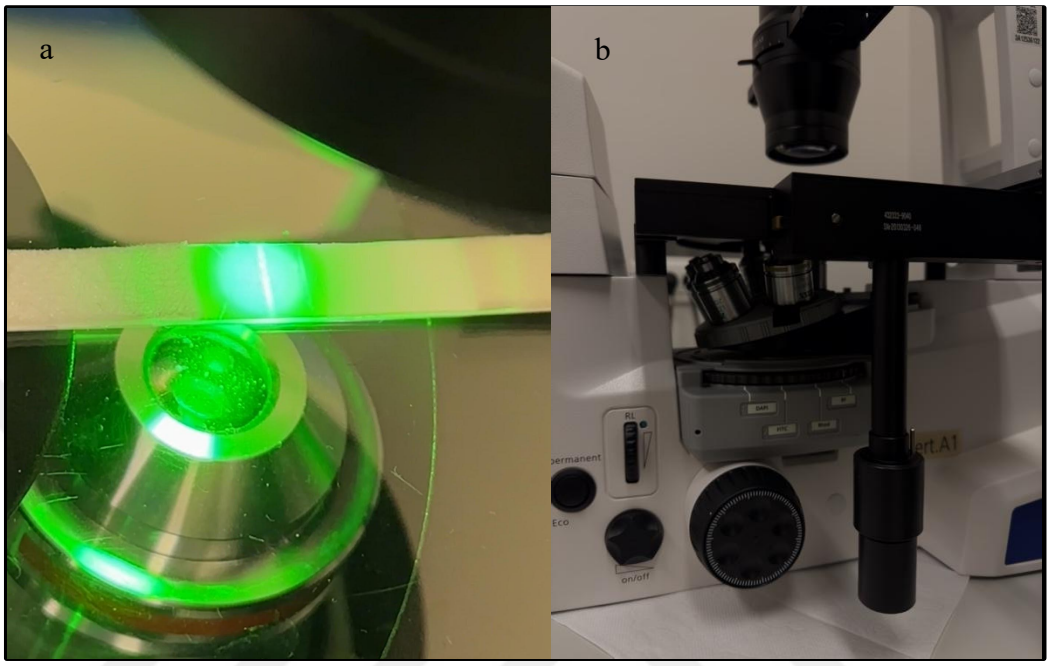


Figure 4.3.1.1. (a) Visualization of the prepared tests under a fluorescent microscope (b) Dyes selected according to the emissions in the microscope used.

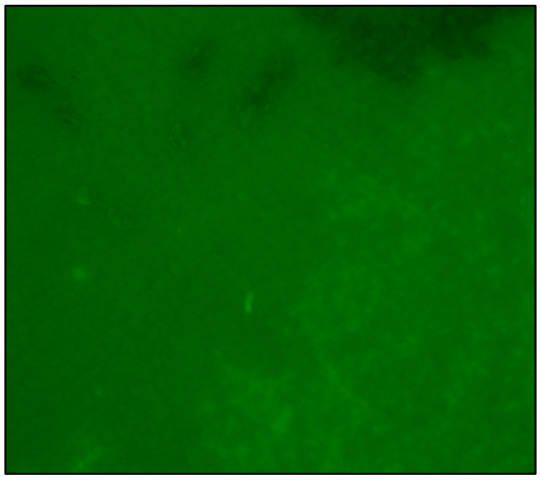

Figure 4.3.1.2. Visualization of the conjugation pad of the prepared negative tests under a fluorescent microscope.

Table 4.3.1.1. (a) Demonstration of test line of prepared positive tests under fluorescence microscope (b) Demonstration of test line of prepared positive tests under fluorescence microscope.

| | **Positive Test Lines** | **Positive Control Lines** |
|---|---|---|
| **1** | a 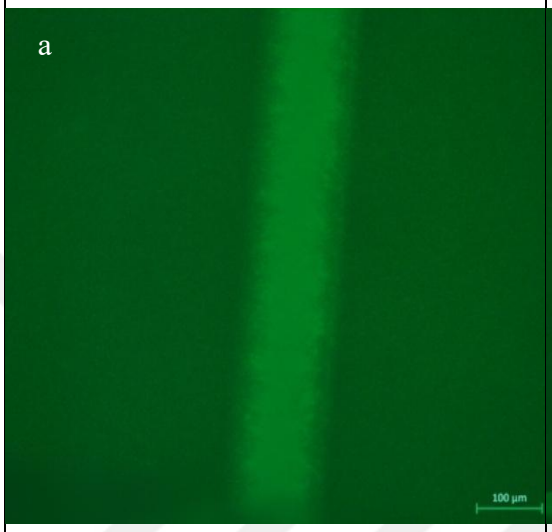  | b 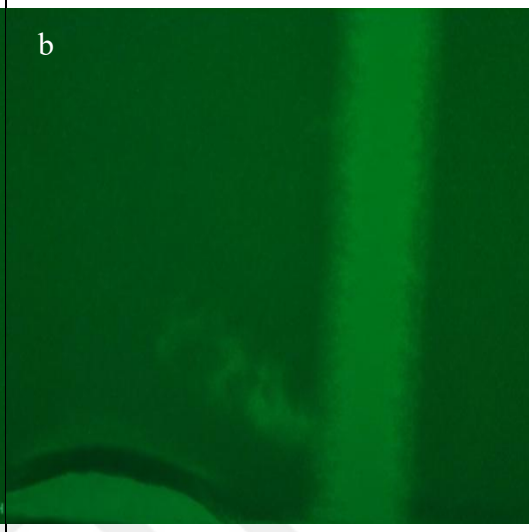 |
| **2** | a 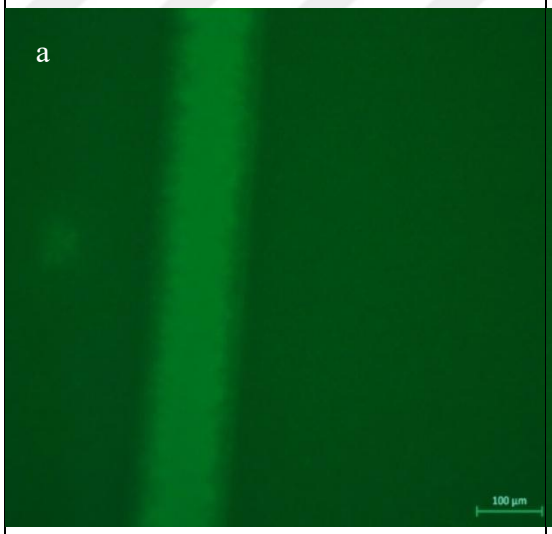  | b 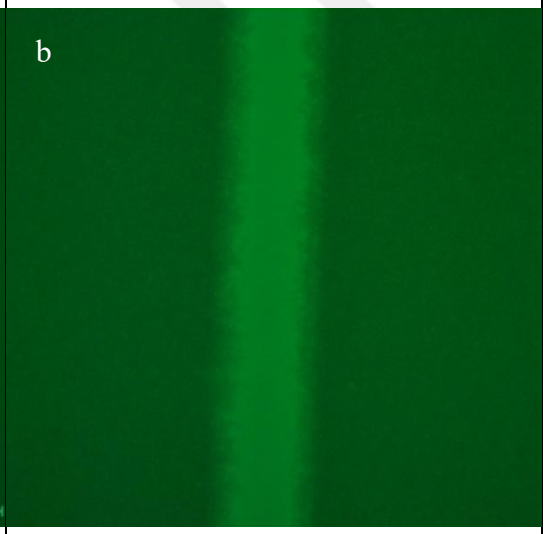 |

| | | |
|---|---|---|
| **3** | 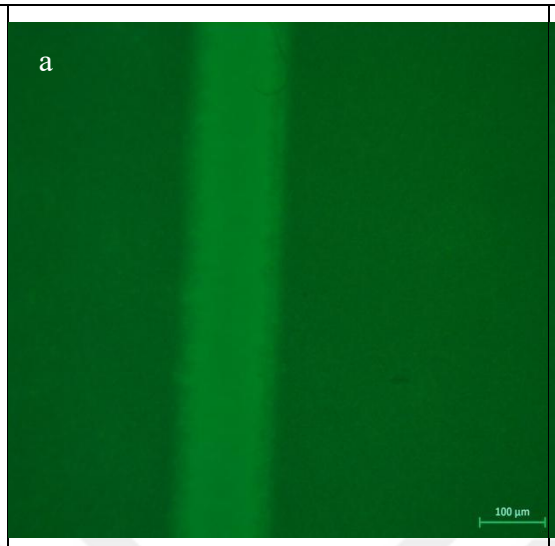 | 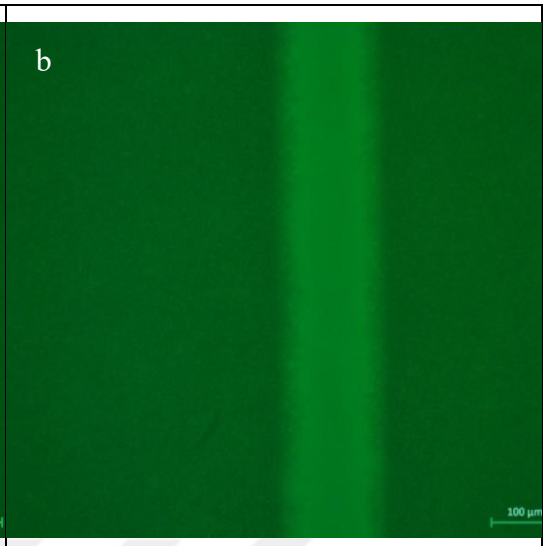 |
| **4** | 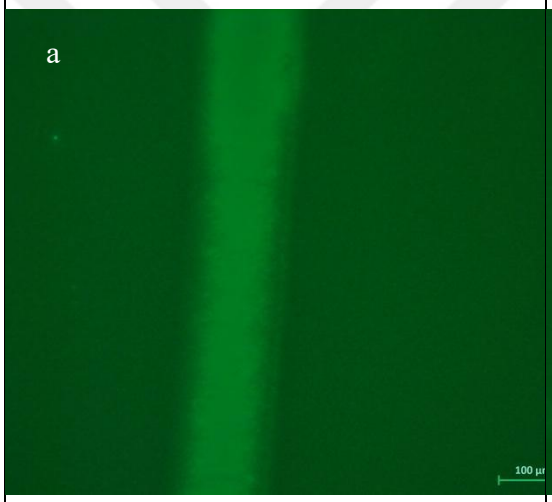 | 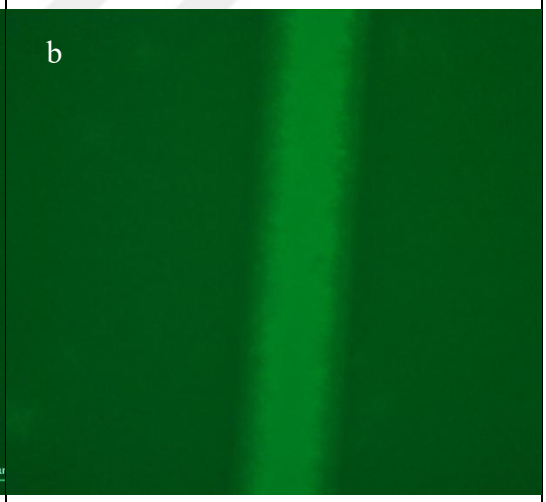 |
| **5** | 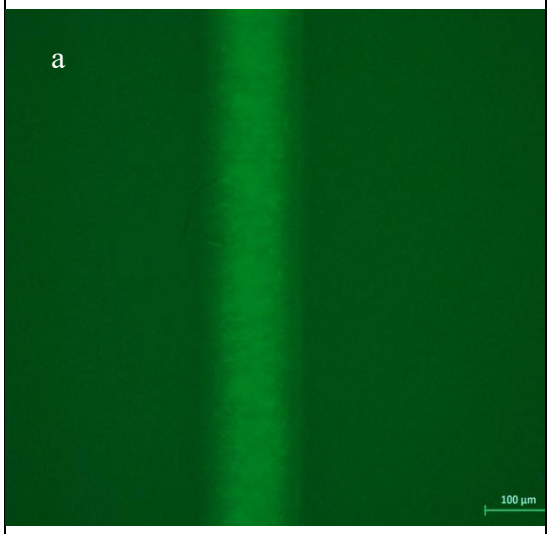 | 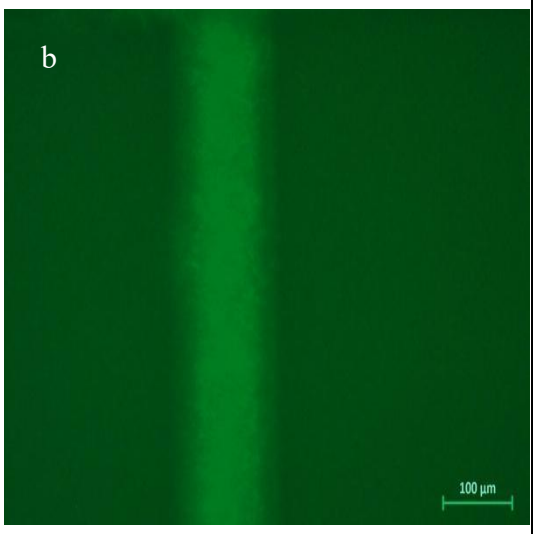 |

| | | |
|---|---|---|
| **6** | a 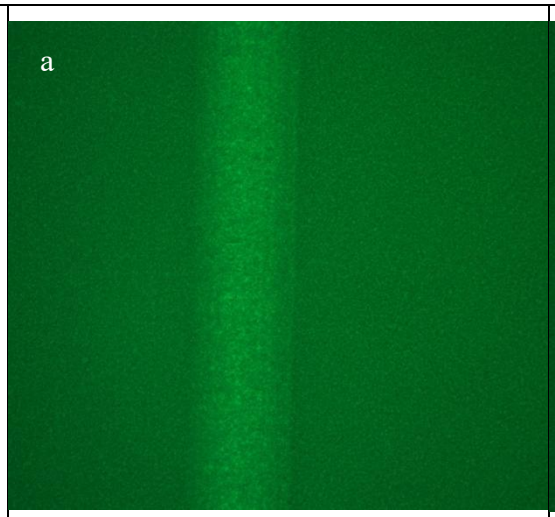 | b 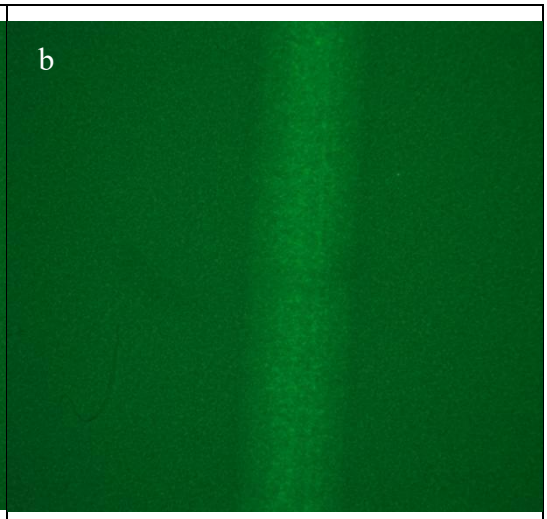 |

Table 4.3.1.2. (a) Demonstration of a negative test prepared under a fluorescent microscope test line. (b1) Demonstration of a negative test prepared under a fluorescent microscope due to the use of high concentration antibodies in the control line. (b2-b3) Demonstration of a negative test prepared under a fluorescent microscope due to the use of low concentration (1:2 ratio) UCNP in the control line at the 30th minute.

| | **Negative Test Lines** | **Negative Control Lines with High and Low Concentrations** |
|---|---|---|
| **1** | a 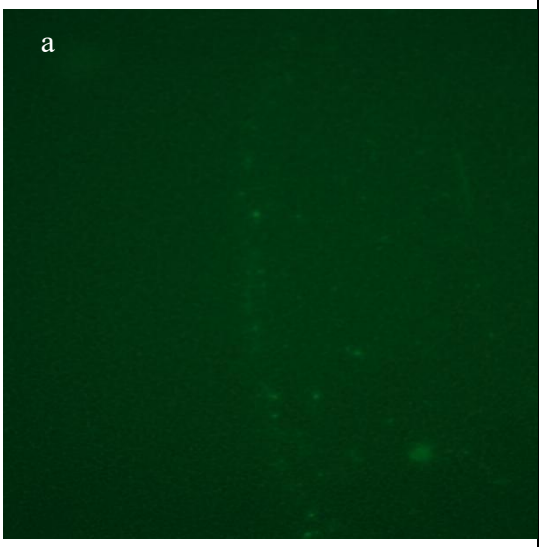 | b1 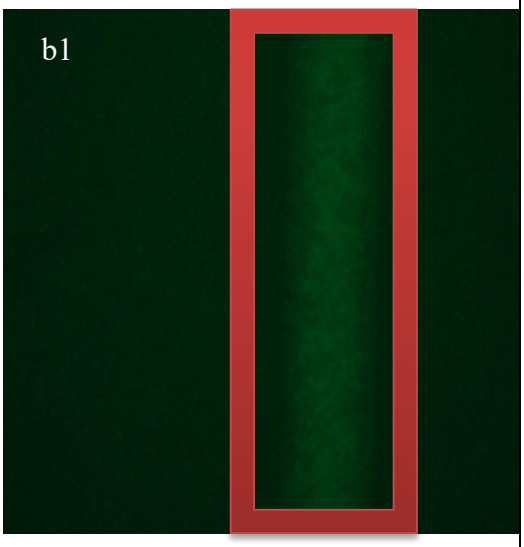 |

| | | |
|---|---|---|
| **2** | 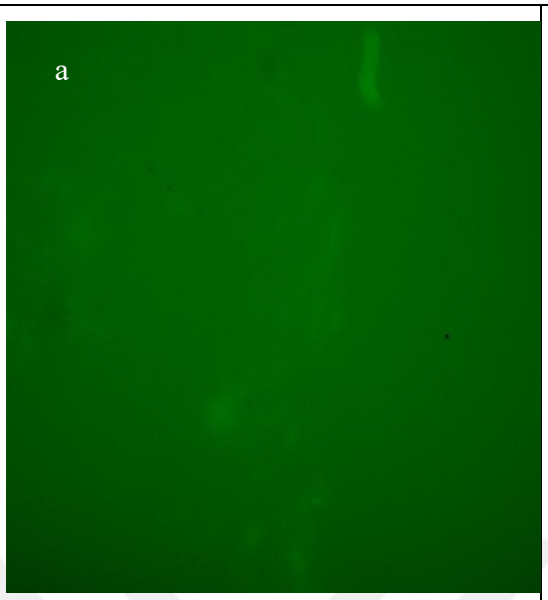  | 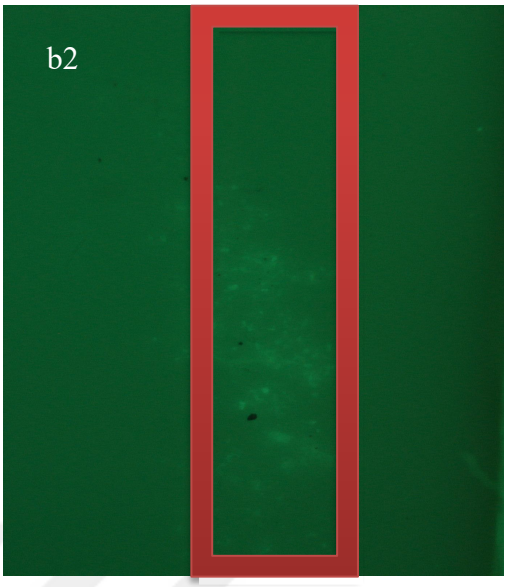  |
| **3** | 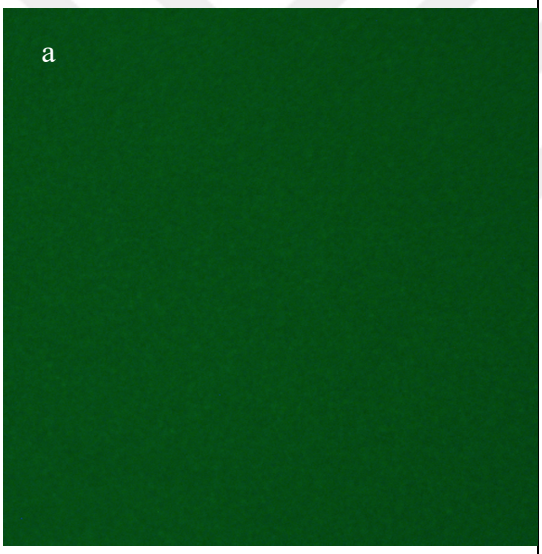  |   |

The control lines of the negative samples are marked with a red frame in table 4.3.1.2. According to the control line marked in b1 is different and more visible than the control lines marked in b2 and b3 is because it depends on the antibody concentrations dispensed on the membrane. The ratio of antibody concentration used in b2 and b3 is 10.2µl - 200 µl PBS. The ratio of antibody concentration used in b1 is 15. 4 µl - 200 µl PBS. Therefore, the optimum antibody concentration value was 15. 4 µl - 200 µl PBS on the control line.

## 4.4. STATISTICAL ANALYSIS

### 4.4.1. Sensitivity and Specificity

In the experiments, streptococcus bacteria as mentioned before in the materials and methods section (section 3.7 bacterial growth) the evaluation of the designed UCNP-based LFA system was carried out by sensitivity and specificity tests. The LFA data obtained from MAT-LAB software. In evaluating the results of a particular test in two populations, one with pathogen and one without pathogen, it is rarely observed perfect discrimination in two groups. For every possible cut-off point or criterion value that is chosen to discriminate between the two populations, some cases with the pathogen are classified as positive (TP = True Positive fraction). Yet, some cases with the pathogen are classified as negative (FN = False Negative fraction). On the other hand, some cases without pathogen can be correctly classified as negative (TN = True Negative fraction), but some cases without pathogen can be classified as positive (FP = False Positive fraction) [57]. Given these possibilities, a perfect test is never positive in a sample without pathogen and never negative in a sample who actually has the pathogen. When evaluating a clinical test, the terms sensitivity and specificity are implemented that are independent of the population of interest subjected to the test. The sensitivity of a clinical test refers to its ability to identify samples with the pathogen accurately, figure 4.4.1.1 [58, 59, 60].

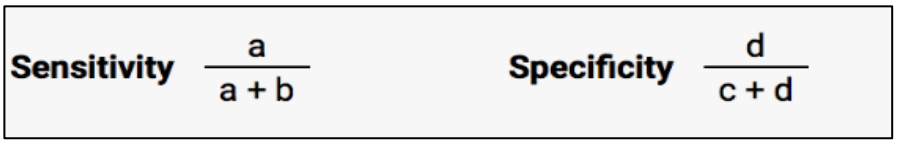


Figure 4.4.1.1. Sensitivity, specificity values formulas [61].

| | Disease | | | | |
|---|---|---|---|---|---|
| **Test** | **Present** | **n** | **Absent** | **n** | **Total** |
| **Positive** | True Positive (TP) | *a* | False Positive (FP) | *c* | *a + c* |
| **Negative** | False Negative (FN) | *b* | True Negative (TN) | *d* | *b + d* |
| **Total** | | *a + b* | | *c + d* | |

Figure 4.4.1.2. Diagram demonstrating the basis for deriving sensitivity, specificity, and positive and negative predictive values. [61].

Table 4.4.1.1. Pathogen Existence

| | **Pathogen** | | | | |
|---|---|---|---|---|---|
| Test | Present | n | Absent | n | Total |
| Positive | True Positive (TP) | A=19 | False Positive (FP) | C=6 | A+C=25 |
| Negative | False Negative (FN) | B=7 | True Negative (TN) | D=18 | B+D=25 |
| Total | | A+B= 26 | | C+D= 24 | |

The test with a sensitivity of 100% correctly identifies all samples who suffer from the pathogen. In the current study all tests examined with a sensitivity in the range of 52.21% to 88.43%, 73.04% of samples truly were detected, shown in table 4.4.1.2. These are named as true positives. The specificity of a test refers to its ability to accurately identify samples without pathogen. Therefore, a test with 100% specificity correctly identifies all samples without the pathogen. A test with a specificity in the range of 53.29% to 90.23%, correctly identifies the 75% of samples without pathogen, named as negative, the test result of these

people is determined as true negative. According to the findings of the sensitivity and specificity of the designed tests, the accuracy was accepted as 74%, given in table 4.4.1.2.

Table 4.4.1.2. Results for sensitivity and specificity [56,57].

| **Statistic** | **Value** | **95% Cl** |
|---|---|---|
| Sensitivity | 73.08% | 52.21% to 88.43% |
| Specificity | 75.00% | 53.29% to 90.23% |
| Accuracy | 74.00% | 59.66% to 85.37% |

The UCNP -based LFA designed and examined within different parameters, shown in Table 4.4.1.3.

Table 4.4.1.3. Parameters for LFA strip

| |
|---|
| **1-** Surface Modification Materials of Nanoparticle<br>a) PAA<br>b) Dopamin |
| **2-** Concentrations of antibodies applied to the Control and Test lines on the Nitrocellulose Membrane |
| **3-** Exchange Efficiency Based on Nitrocellulose Membrane Pore Size |
| **4-** The dispensing speed and the number of repetitions of the lines drawn on the Nitrocellulose Membrane on the device |
| **5-** Materials and Concentrations of buffer solutions applied to the sample pad, conjugation pad and nitrocellulose membrane to increase the sensitivity and capillary flow direction of the designed test. These parameters reduce surface tension, viscosity, and static repulsion. |
| **6-** Depending on Bacteria Concentrations |

According to parameters, optimum bacterial density concentration was found by measuring with a densiometer. A concentration of 105 bacteria was used. The visibility of test lines identified from the Fluorescent Spectrophotometer, and the 15.4µl/200µl antibody concentration was chosen as optimum that was previously mentioned in Table 3.8.4.1.

Table 4.4.1.4. Depending on antibody concentrations

| **Depending on Antibody Concentrations** | | **(18.11.22)** |
|---|---|---|
| 1. antibody | (-) | TRUE NEGATIVE |
| 1. antibody | (-) | FALSE NEGATIVE |
| 1. antibody | (+) | FALSE POSITIVE |
| 1. antibody | (+) | FALSE POSITIVE |
| 2. antibody | (-) | **TRUE NEGATIVE** |
| 2. antibody | (-) | **FALSE NEGATIVE** |
| 2. antibody | (+) | **TRUE POSITIVE** |
| 2. antibody | (+) | **TRUE POSITIVE** |
| 3. antibody | (-) | FALSE NEGATIVE |
| 3. antibody | (-) | FALSE NEGATIVE |
| 3. antibody | (+) | FALSE POSITIVE |
| 3. antibody | (+) | FALSE POSITIVE |

Membrane with a pore size of 8 micrometers was selected according to the visibility of the test and control line that were examined under exposure of a 980 nm laser, Table 4.4.1.5.

Table 4.4.1.5. Depend on membrane pore size

| **Depending on Membrane Pore Size** | | **(09.01.23)** |
|---|---|---|
| 5µ | (-) | FALSE NEGATIVE |
| 5µ | (-) | FALSE NEGATIVE |
| 5µ | (+) | FALSE POSITIVE |
| 5µ | (+) | FALSE POSITIVE |
| 8µ | (-) | **TRUE NEGATIVE** |
| 8µ | (-) | **TRUE NEGATIVE** |
| 8µ | (+) | **TRUE POSITIVE** |
| 8µ | (+) | **FALSE POSITIVE** |
| 10µ | (-) | FALSE NEGATIVE |
| 10µ | (-) | FALSE NEGATIVE |
| 10µ | (+) | TRUE POSITIVE |
| 10µ | (+) | FALSE POSITIVE |

The sensitivity of a LFA test could be enhanced by increasing sample pad thickness that is well reported in the literature [58]. Our findings also confirmed that the thicker (0.6 cm thickness of conjugated pad coded PT-R5) membrane resulted in better sensitivity.

Table 4.4.1.6. Depending on sample pad thickness

| | **Depending on Sample Pad Thickness** | | **(18.01.23)** |
|---|---|---|---|

| 0.35 | | 0.6 | |
|---|---|---|---|
| (+) | TRUE POSITIVE | (+) | **TRUE POSITIVE** |
| (+) | TRUE POSITIVE | (+) | **TRUE POSITIVE** |
| (+) | TRUE POSITIVE | (+) | **TRUE POSITIVE** |
| (+) | TRUE POSITIVE | (+) | **TRUE POSITIVE** |
| (+) | FALSE POSITIVE | (+) | **TRUE POSITIVE** |
| (+) | FALSE POSITIVE | (+) | **TRUE POSITIVE** |
| (+) | FALSE POSITIVE | (+) | **TRUE POSITIVE** |
| (+) | FALSE POSITIVE | (+) | **FALSE POSITIVE** |
| (+) | FALSE POSITIVE | (+) | **FALSE POSITIVE** |
| (+) | FALSE POSITIVE | (+) | **FALSE POSITIVE** |
| (+) | FALSE POSITIVE | (+) | **FALSE POSITIVE** |
| (-) | FALSE NEGATIVE | (-) | **TRUE NEGATIVE** |
| (-) | FALSE NEGATIVE | (-) | **TRUE NEGATIVE** |
| (-) | FALSE NEGATIVE | (-) | **TRUE NEGATIVE** |
| (-) | FALSE NEGATIVE | (-) | **TRUE NEGATIVE** |
| (-) | FALSE NEGATIVE | (-) | **TRUE NEGATIVE** |
| (-) | FALSE NEGATIVE | (-) | **TRUE NEGATIVE** |
| (-) | FALSE NEGATIVE | (-) | **TRUE NEGATIVE** |
| (-) | FALSE NEGATIVE | (-) | **FALSE NEGATIVE** |
| (-) | TRUE NEGATIVE | (-) | **FALSE NEGATIVE** |

| | | | |
|---|---|---|---|
| (-) | TRUE NEGATIVE | (-) | **FALSE NEGATIVE** |
| (-) | TRUE NEGATIVE | (-) | **FALSE NEGATIVE** |

Table 4.4.1.7. Depending on conjugation pad models

| | **Depending on Conjugation Pad Models** | | |
|---|---|---|---|
| R5 | | R7 | |
| (+) | **TRUE POSITIVE** | (+) | FALSE POSITIVE |
| (+) | **TRUE POSITIVE** | (+) | FALSE POSITIVE |
| (+) | **TRUE POSITIVE** | (+) | FALSE POSITIVE |
| (+) | **TRUE POSITIVE** | (+) | FALSE POSITIVE |
| (+) | **FALSE POSITIVE** | (+) | TRUE POSITIVE |
| (-) | **TRUE NEGATIVE** | (-) | FALSE NEGATIVE |
| (-) | **TRUE NEGATIVE** | (-) | FALSE NEGATIVE |
| (-) | **TRUE NEGATIVE** | (-) | FALSE NEGATIVE |
| (-) | **FALSE NEGATIVE** | (-) | TRUE NEGATIVE |
| (-) | **FALSE NEGATIVE** | (-) | TRUE NEGATIVE |

A PBS solution containing 0.5% BSA and 0.05% Tween 20 was used. In the buffer solution preparation of the conjugate pad, borate buffer was used as buffering agents, sucrose as stabilizing and solubilization reagent, BSA as blocking agent and tween 20 as detergents. After these procedures, 10 µl of antibody conjugation solution was added. The membrane was used in 2% BSA, 0.01 M PBS. and 1% - 10% ethanol was used to reduce surface tension,

viscosity and static repulsion. At the end of the period, the membrane was immersed in a wash buffer 0.05% SDS pH 7.4 and 0.005 M PBS.

Depending on the all parameters given in tables 4.4.1.3, optimum results achieved as shown in table 4.4.1.8. Finally, after all the optimization tests completed it is successfully achieved the %100 accuracy.

Table 4.4.1.8. Optimized tests

| **14.04.2023** | **OPTIMUM** |
|---|---|
| (+) | **TRUE POSITIVE** |
| (+) | **TRUE POSITIVE** |
| (+) | **TRUE POSITIVE** |
| (+) | **TRUE POSITIVE** |
| (+) | **TRUE POSITIVE** |
| (-) | **TRUE NEGATIVE** |
| (-) | **TRUE NEGATIVE** |
| (-) | **TRUE NEGATIVE** |
| (-) | **TRUE NEGATIVE** |
| (-) | **TRUE NEGATIVE** |

# 5. CONCLUSION

Infectious diseases caused by pathogenic microorganisms pose a significant risk and are highly contagious, which makes them a critical concern for public health and economy. In today's technology, the rapid, cost effective, and efficient identification of disease that affects humans, especially the prompt detection of viruses, bacteria and parasites within the body, is very crucial.

Point-of-care testing (POCT) plays an important role in providing timely and accurate results to patients in urban areas where central laboratories are not accessible, and to those who receive home care, enabling quickly delivering results and supporting appropriate treatment.

Streptococcus is a common bacterium found in the human flora, especially in the throat and nose, and is prevalent in rural locations where accurate detection may be challenging.

This dissertation is concerned with the development and validation of nanotechnological sensor components and platforms for the diagnosis of A-group beta-hemolytic streptococcus using one of the points of care testing known lateral flow strip (LFA) methods.

Both SEM and TEM observations showed that particles were spherical, and their size were measured to be ~26 nm. In order to make the surface hydrophilic, UCNPs' surfaces were covered with both Dopamine and PAA molecules individually.

According to DLS results, the particle size was found to be 646.1 nm before dopamine coating and their size was increased to 743.9 nm after dopamine coating and for the PAA coated nanoparticle the size observed in 998.1 nm. Although, these results also support the increment in particle size due to dopamine and PAA coating where the findings are not compatible with neither TEM nor XRD. The surface modification of nanoparticles successfully performed and confirmed with FTIR and Zeta Potential analysis. An UCNP based LFA designed and tested using fluorescence microscopy and commercial camera. The design and examinations of UCNP -based LFA were optimized and studied in different parameters including antibody concentrations, membrane pore size and sample pad thickness.

# REFERENCES


1. Ince B, Sezgintürk MK. Lateral flow assays for viruses diagnosis: Up-to-date technology and future prospects. Trends Analyt Chem [Internet]. 2022;157(116725):116725. Available from: http://dx.doi.org/10.1016/j.trac.2022.116725

2. Wang Y, Yu L, Kong X, Sun L. Application of nanodiagnostics in point-of-care tests for infectious diseases. Int J Nanomedicine [Internet]. 2017;12:4789–803. Available from: http://dx.doi.org/10.2147/IJN.S137338

3. Thompson TZ, McMullen AR. Group A streptococcus testing in pediatrics: The move to point-of-care molecular testing. J Clin Microbiol [Internet]. 2020;58(6). Available from: http://dx.doi.org/10.1128/JCM.01494-19

4. Di Nardo F, Cavalera S, Baggiani C, Giovannoli C, Anfossi L. Direct vs mediated coupling of antibodies to gold nanoparticles: The case of salivary cortisol detection by lateral flow immunoassay. ACS Appl Mater Interfaces [Internet]. 2019;11(36):32758–68. Available from: http://dx.doi.org/10.1021/acsami.9b11559

5. Koczula KM, Gallotta A. Lateral flow assays. Essays Biochem [Internet]. 2016;60(1):111–20. Available from: http://dx.doi.org/10.1042/ebc20150012

6. Parolo C, Sena-Torralba A, Bergua JF, Calucho E, Fuentes-Chust C, Hu L, et al. Tutorial: design and fabrication of nanoparticle-based lateral-flow immunoassays. Nat Protoc [Internet]. 2020;15(12):3788–816. Available from: http://dx.doi.org/10.1038/s41596-020-0357-x

7. Steer AC, Danchin MH, Carapetis JR. Group A streptococcal infections in children. J Paediatr Child Health [Internet]. 2007;43(4):203–13. Available from: http://dx.doi.org/10.1111/j.1440-1754.2007.01051.x

8. Eryılmaz M, Acar Soykut E, Çetin D, Boyacı İH, Suludere Z, Tamer U. SERS-based rapid assay for sensitive detection of Group A Streptococcus by evaluation of the swab sampling technique. Analyst [Internet]. 2019;144(11):3573–80. Available from: http://dx.doi.org/10.1039/c9an00173e

9. Goode JA, Rushworth JVH, Millner PA. Biosensor regeneration: A review of common techniques and outcomes. Langmuir [Internet]. 2015;31(23):6267–76. Available from: http://dx.doi.org/10.1021/la503533g

10. Mehrotra P. Biosensors and their applications - A review. J Oral Biol Craniofac Res [Internet]. 2016;6(2):153–9. Available from: http://dx.doi.org/10.1016/j.jobcr.2015.12.002

11. Naresh V, Lee N. A review on biosensors and recent development of nanostructured materials-enabled biosensors. Sensors (Basel) [Internet]. 2021;21(4):1109. Available from: http://dx.doi.org/10.3390/s21041109

12. Welch EC, Powell JM, Clevinger TB, Fairman AE, Shukla A. Advances in biosensors and diagnostic technologies using nanostructures and nanomaterials. Advanced Functional Materials. 2021 Oct;31(44):2104126.

13. Rinken T, editor. Biosensors: Micro and Nanoscale Applications. BoD–Books on Demand; 2015 Sep 24.

14. Haleem A, Javaid M, Singh RP, Suman R, Rab S. Biosensors applications in medical field: A brief review. Sens Int [Internet]. 2021;2(100100):100100. Available from: http://dx.doi.org/10.1016/j.sintl.2021.100100

15. Ajami S, Teimouri F. Features and application of wearable biosensors in medical care. J Res Med Sci [Internet]. 2015;20(12):1208–15. Available from: http://dx.doi.org/10.4103/1735-1995.172991

16. Conroy PJ, Hearty S, Leonard P, O'Kennedy RJ. Antibody production, design and use for biosensor-based applications. Semin Cell Dev Biol [Internet]. 2009;20(1):10–26. Available from: http://dx.doi.org/10.1016/j.semcdb.2009.01.010

17. Gong Y, Zheng Y, Jin B, You M, Wang J, Li X, et al. A portable and universal upconversion nanoparticle-based lateral flow assay platform for point-of-care testing. Talanta [Internet]. 2019;201:126–33. Available from: http://dx.doi.org/10.1016/j.talanta.2019.03.105

18. Bahadır EB, Sezgintürk MK. Lateral flow assays: Principles, designs and labels. Trends Analyt Chem [Internet]. 2016;82:286–306. Available from: http://dx.doi.org/10.1016/j.trac.2016.06.006

19. Zhan S, Lou X, Zhou P, Xia F. Sandwich Assays Based on SPR, SERS, GMR, QCM, Microcantilever, SAW, and RRS Techniques for Protein Detection. In: Biosensors Based on Sandwich Assays. Singapore: Springer Singapore; 2018. p. 69–91.

20. Kaya E, Akata I, Bakırcı S, Dereli D, Küçükgüven E, Yılmaz İ. İMMÜNOKROMATOGRAFİK KART TESTLERİN ÇALIŞMA PRENSİBİ VE ÜRETİM TEKNİKLERİ. Duzce Medical Journal. 2014 Sep 1;16(3).

21. Justino C, Duarte A, Rocha-Santos T. Recent progress in biosensors for environmental monitoring: A review. Sensors (Basel) [Internet]. 2017;17(12):2918. Available from: http://dx.doi.org/10.3390/s17122918

22. Ali J, Najeeb J, Asim Ali M, Farhan Aslam M, Raza A. Biosensors: Their fundamentals, designs, types and most recent impactful applications: A review. J Biosens Bioelectron [Internet]. 2017;08(01). Available from: http://dx.doi.org/10.4172/2155-6210.1000235

23. Neethirajan S, Tuteja SK, Huang S-T, Kelton D. Recent advancement in biosensors technology for animal and livestock health management. Biosens Bioelectron [Internet]. 2017;98:398–407. Available from: http://dx.doi.org/10.1016/j.bios.2017.07.015

24. Encyclopedia of industrial biotechnology: bioprocess, bioseparation, and cell technology. Choice (Middletown) [Internet]. 2010;48(03):48-1218-48–1218. Available from: http://dx.doi.org/10.5860/choice.48-1218

25. Costanzo H, Gooch J, Frascione N. Nanomaterials for optical biosensors in forensic analysis. Talanta [Internet]. 2023;253(123945):123945. Available from: http://dx.doi.org/10.1016/j.talanta.2022.123945

26. Hofstadler SA, Sampath R, Blyn LB, Eshoo MW, Hall TA, Jiang Y, et al. TIGER: the universal biosensor. Int J Mass Spectrom [Internet]. 2005;242(1):23–41. Available from: http://dx.doi.org/10.1016/j.ijms.2004.09.014

27. Tang Z, He C, Tian H, Ding J, Hsiao BS, Chu B, et al. Polymeric nanostructured materials for biomedical applications. Prog Polym Sci [Internet]. 2016;60:86–128. Available from: http://dx.doi.org/10.1016/j.progpolymsci.2016.05.005

28. Yue Q, Wang M, Sun Z, Wang C, Wang C, Deng Y, et al. A versatile ethanol-mediated polymerization of dopamine for efficient surface modification and the construction of functional core-shell nanostructures. J Mater Chem B Mater Biol Med [Internet]. 2013;1(44):6085–93. Available from: http://dx.doi.org/10.1039/c3tb21028f

29. Huang X, Aguilar ZP, Xu H, Lai W, Xiong Y. Membrane-based lateral flow immunochromatographic strip with nanoparticles as reporters for detection: A review. Biosens Bioelectron [Internet]. 2016;75:166–80. Available from: http://dx.doi.org/10.1016/j.bios.2015.08.032

30. You S-M, Luo K, Jung J-Y, Jeong K-B, Lee E-S, Oh M-H, et al. Gold nanoparticle-coated starch magnetic beads for the separation, concentration, and SERS-based detection of E. coli O157:H7. ACS Appl Mater Interfaces [Internet]. 2020;12(16):18292–300. Available from: http://dx.doi.org/10.1021/acsami.0c00418

31. Mohanraj VJ, Chen Y. Nanoparticles - A review. Trop J Pharm Res [Internet]. 2007;5(1). Available from: http://dx.doi.org/10.4314/tjpr.v5i1.14634

32. Niedbala RS, Vail TL, Feindt H, Li S, Burton JL. Multiphoton up-converting phosphors for use in rapid immunoassays. In: Cohn GE, editor. In-Vitro Diagnostic Instrumentation. SPIE; 2000.

33. He H, Liu B, Wen S, Liao J, Lin G, Zhou J, et al. Quantitative lateral flow strip sensor using highly doped upconversion nanoparticles. Anal Chem [Internet]. 2018;90(21):12356–60. Available from: http://dx.doi.org/10.1021/acs.analchem.8b04330

34. Controlled synthesis of NaYF4: Yb, Er upconversion nanocrystals as potential probe for bioimaging: a focus on heat treatment.

35. Hasirci V, Hasirci N. Fundamentals of Biomaterials. 1st ed. New York, NY: Springer; 2018.

36. Sharma SK, editor. Handbook of materials characterization. 1st ed. Basel, Switzerland: Springer International Publishing; 2018.

37. Scognamiglio F, Travan A, Rustighi I, Tarchi P, Palmisano S, Marsich E, et al. Adhesive and sealant interfaces for general surgery applications: Adhesive and sealant interfaces for general surgery applications. J Biomed Mater Res B Appl Biomater [Internet]. 2016;104(3):626–39. Available from: http://dx.doi.org/10.1002/jbm.b.33409

38. Shukla NB, Daraboina N, Madras G. Oxidative and photooxidative degradation of poly(acrylic acid). Polym Degrad Stab [Internet]. 2009;94(8):1238–44. Available from: http://dx.doi.org/10.1016/j.polymdegradstab.2009.04.020

39. Yang JM, Huang MJ, Yeh TS. Preparation of poly(acrylic acid) modified polyurethane membrane for biomaterial by UV radiation without degassing. J Biomed Mater Res [Internet]. 1999;45(2):133–9. Available from: http://dx.doi.org/10.1002/(sici)1097-4636(199905)45:2<133::aid-jbm8>3.0.co;2-d

40. Saroj S, Rajput SJ. Tailor-made pH-sensitive polyacrylic acid functionalized mesoporous silica nanoparticles for efficient and controlled delivery of anti-cancer drug Etoposide. Drug Dev Ind Pharm [Internet]. 2018;44(7):1198–211. Available from: http://dx.doi.org/10.1080/03639045.2018.1438467

41. Electrospinning ethanol-water solutions of poly (acrylic acid): Nonlinear viscosity variations and dynamic Taylor cone behavior.

42. Jiang J, Zhu L, Zhu L, Zhu B, Xu Y. Surface characteristics of a self-polymerized dopamine coating deposited on hydrophobic polymer films. Langmuir [Internet]. 2011;27(23):14180–7. Available from: http://dx.doi.org/10.1021/la202877k

43. Park J, Brust TF, Lee HJ, Lee SC, Watts VJ, Yeo Y. Polydopamine-based simple and versatile surface modification of polymeric nano drug carriers. ACS Nano [Internet]. 2014;8(4):3347–56. Available from: http://dx.doi.org/10.1021/nn405809c

44. Macit HB, Macit G, Güngör O. SOSYAL MEDYA BAĞIMLILIĞI VE DOPAMİN ODAKLI GERİBİLDİRİM ÜZERİNE BİR ARAŞTIRMA. Mehmet Akif Ersoy Üniv

İktis ve İdari Bilim Fak derg [Internet]. 2018;5(3):882–97. Available from: http://dx.doi.org/10.30798/makuiibf.435845

45. Brangel P, Sobarzo A, Parolo C, Miller BS, Howes PD, Gelkop S, et al. A serological point-of-care test for the detection of IgG antibodies against Ebola virus in human survivors. ACS Nano [Internet]. 2018;12(1):63–73. Available from: http://dx.doi.org/10.1021/acsnano.7b07021

46. Pleiner T, Bates M, Görlich D. A toolbox of anti–mouse and anti–rabbit IgG secondary nanobodies. J Cell Biol [Internet]. 2018;217(3):1143–54. Available from: http://dx.doi.org/10.1083/jcb.201709115

47. Forthal DN, Landucci G, Gorny MK, Zolla-Pazner S, Robinson WE Jr. Functional activities of 20 human immunodeficiency virus type 1 (HIV-1)-specific human monoclonal antibodies. AIDS Res Hum Retroviruses [Internet]. 1995;11(9):1095–9. Available from: http://dx.doi.org/10.1089/aid.1995.11.1095

48. Chames P, Van Regenmortel M, Weiss E, Baty D. Therapeutic antibodies: successes, limitations and hopes for the future: Therapeutic antibodies: an update. Br J Pharmacol [Internet]. 2009;157(2):220–33. Available from: http://dx.doi.org/10.1111/j.1476-5381.2009.00190.x

49. Norton LE, Lee BR, Harte L, Mann K, Newland JG, Grimes RA, et al. Improving guideline-based streptococcal pharyngitis testing: A quality improvement initiative. Pediatrics [Internet]. 2018;142(1). Available from: http://dx.doi.org/10.1542/peds.2017-2033

50. Cohen JF, Bertille N, Cohen R, Chalumeau M. Rapid antigen detection test for group A streptococcus in children with pharyngitis. Cochrane Database Syst Rev [Internet]. 2016;7(7):CD010502. Available from: http://dx.doi.org/10.1002/14651858.CD010502.pub2

51. Eryılmaz M, Tamer U, Boyacı İH. Nanoparticle-assisted pyrrolidonyl arylamidase assay for a culture-free Group A Streptococcus pyogenes detection with image analysis. Talanta [Internet]. 2020;212(120781):120781. Available from: http://dx.doi.org/10.1016/j.talanta.2020.120781

52. Güler M. Güncellenen kılavuz sonrasında ilk atak akut romatizmal ateş tanısı alan çocuk hastaların klinik özellikleri. Turk Pediatri Ars [Internet]. 2019; Available from: http://dx.doi.org/10.14744/turkpediatriars.2019.69376

53. Carapetis JR, Steer AC, Mulholland EK, Weber M. The global burden of group A streptococcal diseases. Lancet Infect Dis [Internet]. 2005;5(11):685–94. Available from: http://dx.doi.org/10.1016/S1473-3099(05)70267-X

54. Vojdani A, Turnpaugh CC. Antibodies against Group A Streptococcus, dopamine receptors, and ganglioside GM1 cross-react with a variety of food antigens, potentially interfering with biomarkers for PANS and PANDAS. Biomark Neuropsychiatry [Internet]. 2020;3(100023):100023. Available from: http://dx.doi.org/10.1016/j.bionps.2020.100023

55. Bailes J, Mayoss S, Teale P, Soloviev M. Gold nanoparticle antibody conjugates for use in competitive lateral flow assays. Methods Mol Biol [Internet]. 2012;906:45–55. Available from: http://dx.doi.org/10.1007/978-1-61779-953-2_4

56. Liu J, Jalali M, Mahshid S, Wachsmann-Hogiu S. Are plasmonic optical biosensors ready for use in point-of-need applications? Analyst [Internet]. 2020;145(2):364–84. Available from: http://dx.doi.org/10.1039/c9an02149c

57. Swift A, Heale R, Twycross A. What are sensitivity and specificity? Evid Based Nurs [Internet]. 2020;23(1):2–4. Available from: http://dx.doi.org/10.1136/ebnurs-2019-103225

58. Clinical tests: sensitivity and specificity Abdul Ghaaliq Lalkhen MB ChB FRCA Anthony McCluskey BSc MB ChB FRCA.

59. Hajian-Tilaki K. Receiver operating characteristic (ROC) curve analysis for medical diagnostic test evaluation. Caspian J Intern Med. 2013 Spring;4(2):627–35.

60. Mitchell MD. Validation of the summary ROC for diagnostic test meta-analysis: a Monte Carlo simulation. Acad Radiol [Internet]. 2003;10(1):25–31. Available from: http://dx.doi.org/10.1016/s1076-6332(03)80784-5

61. Schoonjans F. ROC curve analysis [Internet]. MedCalc. MedCalc Software; 2022 [cited 2023 May 12]. Available from: https://www.medcalc.org/manual/roc-curves.php